



Cite this: *RSC Adv.*, 2022, **12**, 35158

Received 7th November 2022
 Accepted 30th November 2022

DOI: 10.1039/d2ra07056a
rsc.li/rsc-advances

1 Introduction

Multicomponent reactions (MCRs) are convergent reactions that lead to a single product from three or more reactants, where all or most of these atoms are incorporated in the product structure through a cascade of elementary reactions.^{1–3} The popularity of MCRs lies in the operational simplicity, savings in time and energy (step efficiency), proceeding with high convergence (process efficiency) and bond-forming index (BFI), and compatibility with a range of unprotected orthogonal

*Grupo de Catálisis de la UPTC, Escuela de Ciencias Química, Universidad Pedagógica y Tecnológica de Colombia, Avenida Central del Norte 39-115, Tunja, Colombia.
 E-mail: diana.becerra08@uptc.edu.co; juan.castillo06@uptc.edu.co*



Diana Hurtado-Rodríguez was born in Manizales (Colombia) and received her BSc degree at the Universidad Pedagógica y Tecnológica de Colombia (Tunja) in 2023. Currently, she is working on her MSc degree in Chemistry under the supervision of Dr Juan Castillo, Dr Diana Becerra and Prof. Hugo Rojas at the Universidad Pedagógica y Tecnológica de Colombia (Tunja). Her research focuses on the synthesis of 2-pyridone derivatives with potential anticancer activity.

functional groups.^{1–3} Thereby, MCRs are considered a powerful alternative to prepare structurally complex and diverse organic molecules with a wide range of applications in polymer chemistry,⁴ combinational chemistry,⁵ organic chemistry,^{6,7} medicinal chemistry,^{3,8} and chiefly drug discovery programs.⁹ Many of the classical MCRs are named reactions and all have allowed the incorporation of bioactive scaffold shapes, including Strecker (1850),¹⁰ Hantzsch (1881),¹¹ Biginelli (1891),¹² Mannich (1912),¹³ Passerini (1921),¹⁴ Kabachnik-Fields (1952),¹⁵ Asinger (1956),¹⁶ Ugi (1959),¹⁷ Gewald (1966),¹⁸ Van Leusen (1977),¹⁹ and Groebke-Blackburn-Bienaymé (1998).²⁰ Over the past few decades, MCRs have been employed as a powerful tool to create chemical diversity, high throughput generation of bioactive scaffolds, and the large-scale production of drug candidates.^{21,22}



Angélica Salinas-Torres was born in Tunja (Colombia) and received her BSc degree at the Universidad Pedagógica y Tecnológica de Colombia (Tunja) in 2021. Currently, she is working on her MSc degree in Chemistry under the supervision of Dr Juan Castillo, Dr Diana Becerra and Prof. Hugo Rojas at the Universidad Pedagógica y Tecnológica de Colombia (Tunja). Her research focuses on the synthesis of amides with potential anticancer activity.



It is estimated that roughly 5% of the marketed drugs have been synthesized through an MCR strategy, including Nifedipine (Hantzsch), Telaprevir (Passerini), and Crixivan (Ugi).²²

Among all the synthetic and naturally occurring N-heterocycles, 2(1*H*)-pyridones are six-membered heterocycles possessing C=O and NH groups, which have been employed as privileged scaffolds in medicinal chemistry and drug discovery programs due to their interesting structural features and a broad range of biological activities.^{23–25} The most important structural characteristic is the tautomeric equilibrium between 2-hydroxypyridine (lactim) and 2(1*H*)-pyridone (lactam), which predominates in both solid and solution phases.^{26–28} Additionally, 2(1*H*)-pyridones are important in drug design due to their capability to: (a) act as bioisosteres for amides, phenyls, pyridines, pyridine *N*-oxides, and phenols; (b) serve as both hydrogen bond donors and/or acceptors; and (c) achieve better drug-like properties such as low lipophilicity, solubility in



Hugo Rojas was born in Tunja (Colombia). He is a Full Professor at the School of Chemical Sciences at the Universidad Pedagógica y Tecnológica de Colombia (Tunja), leading the Grupo de Catalysis de la UPTC since 1996. He completed his PhD in Chemical Sciences under the supervision of Prof. Patricio Reyes at the Universidad de Concepción (Chile) in 2003. His current research interests involve the areas of heterogeneous catalysis, biocatalysis, photocatalysis, catalysis in organic chemistry, and materials chemistry.

Damien Bonne. In 2017, she began her academic career at the Universidad Pedagógica y Tecnológica de Colombia (Tunja). Her research interest focuses on the synthesis of biologically active heterocyclic compounds, sustainable chemistry, catalysis in organic chemistry, and supramolecular chemistry.



Diana Becerra was born in Florida (Colombia). After studying Chemistry at the Universidad del Valle (Cali, Colombia), she received her PhD in Chemical Sciences in 2014 under the supervision of Prof. Braulio Insuasty. Then, she became a postdoctoral fellow at the Institut des Sciences Moléculaires de Marseille (France) under the supervision of Prof. Jean Rodriguez and Prof.

Juan Castillo. After studying Chemistry at the Universidad del Valle (Cali, Colombia), he received his PhD in Chemical Sciences in 2013 under the supervision of Prof. Rodrigo Abonia. He became a postdoctoral fellow at the Institut des Sciences Moléculaires de Marseille (France) under the supervision of Prof. Jean Rodriguez and Prof. Yoann Coquerel. Later, he was a postdoctorate researcher at the Universidad de los Andes (Bogotá, Colombia) under the supervision of Prof. Jaime Portilla. In 2018, he began his academic career at the Universidad Pedagógica y Tecnológica de Colombia (Tunja). His current research interests involve the synthesis of biologically active heterocyclic compounds, sustainable chemistry, catalysis in organic chemistry, and supramolecular chemistry.

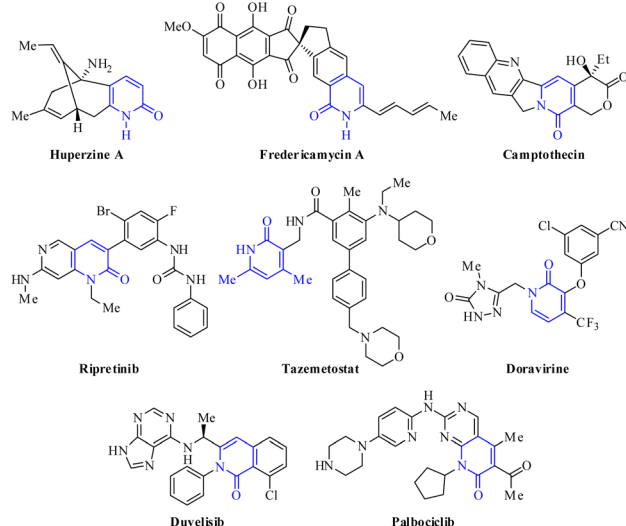


Fig. 1 Bioactive natural products and selected examples of FDA-approved drugs containing 2-pyridone core.

water, and metabolic stability under physiological conditions.^{29,30} For instance, 2-pyridone is widely found in bioactive natural products, including Huperzine A used in China as a treatment for Alzheimer's disease and is available in the U.S. as a nutraceutical (not regulated by the FDA),³¹ fredericamycin A employed as a novel lead compound for the chemotherapy of human cancers,³² and Camptothecin displayed anticancer activity as an inhibitor of DNA topoisomerase I (Fig. 1).³³ Over the past two decades, 2-pyridone derivatives have become a hot point in drug discovery programs with an increasing number of FDA-approved drugs as kinase inhibitors, including the most recent approvals of Ripretinib (2020), Tazemetostat (2020), Doravirine (2018), Duvelisib (2018), and Palbociclib (2015)



Juan Castillo was born in Cali (Colombia). After studying Chemistry at the Universidad del Valle (Cali, Colombia), he received his PhD in Chemical Sciences in 2013 under the supervision of Prof. Rodrigo Abonia. He became a postdoctoral fellow at the Institut des Sciences Moléculaires de Marseille (France) under the supervision of Prof. Jean Rodriguez and Prof. Yoann Coquerel.

Later, he was a postdoctorate researcher at the Universidad de los Andes (Bogotá, Colombia) under the supervision of Prof. Jaime Portilla. In 2018, he began his academic career at the Universidad Pedagógica y Tecnológica de Colombia (Tunja). His current research interests involve the synthesis of biologically active heterocyclic compounds, sustainable chemistry, catalysis in organic chemistry, and supramolecular chemistry.



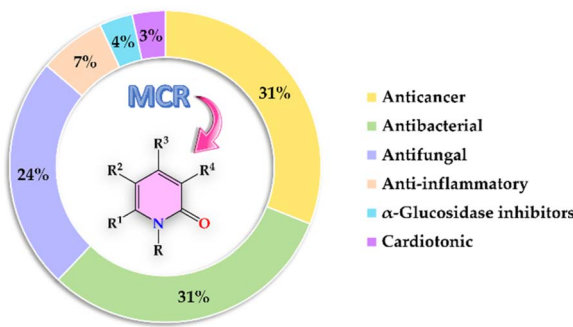


Fig. 2 Bibliometric graphic depicting the percentage of articles associated with each biological activity screened from 1999 to date [data were collected searching in Scopus for the keywords: "2-pyridones", "biological activity", and "multicomponent reactions"].

(Fig. 2).²⁹ In particular, tazemetostat is a potent, selective, and orally bioavailable small-molecule inhibitor of EZH2. Thereby, EZH2 inhibitors represent a notable clinical promise for cancer treatment because some anticancer drugs have acquired resistance and suffer from poor bio-distribution and limited brain penetration.³⁴

The present review covers articles published from 1999 to date related to anticancer, antibacterial, antifungal, anti-inflammatory, α -glucosidase inhibitor, and cardiotonic activities of 2-pyridones derivatives obtained exclusively by an MCR (Fig. 2). It should be noted that 86% of articles found suitable for this review corresponded to 2-pyridone derivatives with anticancer (31%), antibacterial (31%), and antifungal (24%)

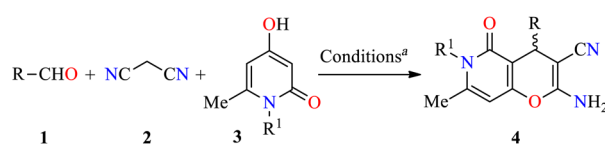
activities. For a better comprehension, the present review has been organized and discussed in terms of the biological activities exhibited by 2-pyridone derivatives.

2 Multicomponent synthesis of bioactive 2-pyridone derivatives

2.1. Anticancer activity

Analysis of the database of U.S. FDA-approved drugs reveals that nearly 60% of unique small-molecule drugs contain an N-heterocycle.³⁵ In particular, N-heterocyclic skeletons are used as building blocks for the production of oncology-active pharmaceutical ingredients (APIs) and many biologically active molecules.³⁶ As a result, a plethora of methodologies for preparing diversely functionalized N-heterocycles with important anti-cancer activity have been described during the last decade.^{37–40} In this regard, Magedov *et al.* described the synthesis of pyrano[3,2-*c*]pyridones 4 through a three-component reaction of diverse aromatic aldehydes 1, malononitrile 2, and 4-hydroxy-1,6-dimethylpyridin-2(1*H*)-one 3 mediated by triethylamine (45 mol%) in refluxing ethanol for 50 min (Table 1).⁴¹ The reaction mixture was cooled at room temperature, and the precipitate was filtered and washed with ethanol to afford products 4a–l in 75–98% yields. This protocol was distinguished by its short reaction times, high yields, the use of a green solvent, and broad substrate scope. Moreover, compounds 4a–l were screened for their anticancer activity against HeLa (cervical cancer) cell line. The cells were treated with respective compounds for 48 h and cell viability was assessed through

Table 1 Three-component synthesis and anticancer evaluation of pyrano[3,2-*c*]pyridones 4



Compound	R	R ¹	Yield 4 (%)	IC ₅₀ ^b (μM)
4a	3-Br-4-NMe ₂ C ₆ H ₃	Me	83	0.33 ± 0.06
4b	3-Br-4,5-(MeO) ₂ C ₆ H ₂	Me	87	0.58 ± 0.14
4c	3-Br-4-EtO-5-MeOC ₆ H ₂	Me	88	1.08 ± 0.8
4d	3-Br-4-OH-5-MeOC ₆ H ₂	Me	75	2.67 ± 1.1
4e	3-Br-4-AcO-5-MeOC ₆ H ₂	Me	83	3.50 ± 1.3
4f	3-Br-4-F-C ₆ H ₃	Me	84	6.33 ± 1.1
4g	3-BrC ₆ H ₄	Me	97	6.50 ± 1.3
4h	3,4-(Cl) ₂ C ₆ H ₃	Me	98	18.3 ± 2.9
4i	3,4,5-(MeO) ₃ C ₆ H ₂	Me	97	43.3 ± 5.1
4j	4-iPrC ₆ H ₄	Me	81	>100
4k	3-NO ₂ C ₆ H ₄	Me	97	35.0 ± 21.8
4l	3,4,5-(MeO) ₃ C ₆ H ₂	3,4-Dimethoxyphenethyl	80	22.7 ± 6.4

^a Reaction conditions: aldehyde 1 (0.8 mmol), malononitrile 2 (0.8 mmol), 4-hydroxy-1,6-dimethylpyridin-2(1*H*)-one 3 (0.8 mmol), triethylamine (45 mol%), EtOH (3 mL), reflux, 50 min. ^b Compound concentration required to reduce HeLa cell viability by 50% after 48 h treatment relative to 100% DMSO control as assessed with the MTT assay. Data shown are average ± SD of three independent experiments.



Table 2 Flow cytometric cell cycle analysis of Jurkat cells

Compound	% Relative DNA content ^a		
	G ₀ /G ₁	S	G ₂ /M
DMSO	49.4 ± 2.7	26.6 ± 0.1	23.9 ± 2.4
4a (5 μM)	14.4 ± 1.7	18.1 ± 0.6	67.5 ± 2.3
4b (5 μM)	12.0 ± 3.5	19.0 ± 2.0	68.5 ± 4.7
Colchicine (25 μM)	19.0 ± 0.2	23.1 ± 0.1	57.9 ± 0.1

^a % Relative DNA content ± SD after 15 h treatment of Jurkat cells with indicated compounds from two independent experiments.

measurements of mitochondrial dehydrogenase activity using the MTT method (Table 1). Data shown are average ± SD of three independent experiments. These compounds showed good to excellent anticancer activity with IC₅₀ values ranging from 0.33 to >100 μM. Remarkably, compounds **4a** (R = 3-Br-4-NMe₂C₆H₃, R¹ = Me) and **4b** (R = 3-Br-4,5-(MeO)₂C₆H₂, R¹ = Me) displayed the best activity with IC₅₀ values of 0.33 and 0.58

μM, respectively. Since many clinically used anticancer agents induce apoptosis in cancer cells, pyrano[3,2-*c*]pyridones **4a–i** and **4l** were tested for their ability to induce apoptosis in the Jurkat cells using a flow cytometric annexin-V/propidium iodide assay. In summary, the compounds **4a–g** were found to be strong inducers of apoptosis (50–60% after 36 h treatment) in Jurkat cells at 5 μM concentration, which is comparable to the Colchicine used at the same concentration. Lastly, the flow cytometric cell cycle analysis was performed with compounds **4a** and **4b** against the Jurkat cell line, leading to a pronounced cell cycle arrest in the G₂/M phase (Table 2). This result is characteristic of antimitotic agents disrupting microtubule assembly, which is also observed with 2-amino-4-aryl-4*H*-chromene-3-carbonitriles that bind to or near the colchicine binding site on β-tubulin.⁴²

In a similar way to previously described,⁴¹ Magedov *et al.* reported the synthesis of pyrano[3,2-*c*]quinolones **6a–y** in 64–97% yields *via* a three-component approach utilizing commercially available 4-hydroxy-1-methylquinolin-2(1*H*)-one **5** under

Table 3 Three-component synthesis and anticancer evaluation of pyrano[3,2-*c*]quinolones **6**

Compound	R	Yield 6 (%)	GI ₅₀ ^b (μM)	
			HeLa	MCF-7
6a	C ₆ H ₅	78	0.39 ± 0.01	3.38 ± 0.53
6b	3,4,5-(MeO) ₃ C ₆ H ₂	86	0.24 ± 0.02	1.0 ± 0.3
6c	3-OH-4-MeOC ₆ H ₃	82	>50	>50
6d	3-MeO-4-OHC ₆ H ₃	84	0.63 ± 0.05	0.5 ± 0.14
6e	3-MeO-4-OH-5-NO ₂ C ₆ H ₂	89	0.63 ± 0.02	0.71 ± 0.12
6f	3-NO ₂ C ₆ H ₄	77	0.32 ± 0.02	1.1 ± 0.1
6g	2-NO ₂ C ₆ H ₄	73	5.0 ± 1.4	3.5 ± 0.3
6h	4-Pyridinyl	79	>50	32 ± 2
6i	3-Pyridinyl	81	2.0 ± 0.1	>50
6j	2-Furanyl	75	22 ± 1	35 ± 2
6k	5-Methyl-2-furanyl	78	3.9 ± 0.2	5.1 ± 0.1
6l	2,3-(Cl) ₂ C ₆ H ₃	95	1.8 ± 0.2	>50
6m	2,6-(Cl) ₂ C ₆ H ₃	88	>50	36 ± 2
6n	3,4-(Cl) ₂ C ₆ H ₃	97	0.3 ± 0.03	2.5 ± 0.3
6o	3-ClC ₆ H ₄	91	0.15 ± 0.04	2.2 ± 0.2
6p	3-FC ₆ H ₄	90	0.30 ± 0.01	1.0 ± 0.3
6q	3-BrC ₆ H ₄	93	0.74 ± 0.03	0.003 ± 0.001
6r	3-Br-4-FC ₆ H ₃	95	0.27 ± 0.03	0.81 ± 0.08
6s	3,5-(Br) ₂ -4-OHC ₆ H ₂	92	0.27 ± 0.02	0.43 ± 0.01
6t	3-Br-4-OH-5-MeOC ₆ H ₂	94	0.047 ± 0.01	0.39 ± 0.16
6u	3-Br-4,5-(MeO) ₂ C ₆ H ₂	95	0.014 ± 0.003	0.38 ± 0.03
6v	3,5-(Br) ₂ C ₆ H ₃	82	0.077 ± 0.006	0.075 ± 0.007
6w	3-Br-4-MeOC ₆ H ₃	64	0.41 ± 0.04	0.5 ± 0.1
6x	5-Bromopyridin-3-yl	85	0.013 ± 0.003	0.015 ± 0.008
6y	3-Br-4-AcO-5-MeOC ₆ H ₂	84	0.18 ± 0.02	0.025 ± 0.06

^a Reaction conditions: aldehyde **1** (0.8 mmol), malononitrile **2** (0.8 mmol), 4-hydroxy-1-methylquinolin-2(1*H*)-one **5** (0.8 mmol), triethylamine (45 mol%), EtOH (3 mL), reflux, 50 min. ^b Compound concentration required to reduce HeLa and MCF-7 cells viability by 50% after 48 h treatment relative to 100% DMSO control as assessed with the MTT assay. Data shown are average ± SD of two independent experiments.



Table 4 Flow cytometric cell cycle analysis of Jurkat cells

Compound	% Relative DNA content ^a		
	G ₀ /G ₁	S	G ₂ /M
DMSO	56 ± 2	21 ± 3	20 ± 2
6t	27 ± 3	22 ± 2	47 ± 3
6u	20 ± 2	28 ± 2	49 ± 2

^a % Relative DNA content ± SD after 24 h treatment of Jurkat cells with indicated compounds from two independent experiments. Compounds **6t** and **6u** are used at 1 μ M employing the flow cytometric Vybrant Orange staining assay.

the same reaction conditions (Table 3).⁴³ The anticancer activity of all synthesized compounds was evaluated against HeLa (cervical cancer) and MCF-7 (breast cancer) cell lines. The cells were treated with respective compounds for 48 h, and cell viability was assessed through measurements of mitochondrial dehydrogenase activity using the MTT method (Table 3). Data shown are average ± SD of two independent experiments. Overall, compounds **6a–y** showed excellent activity against HeLa and MCF-7 cancer cell lines with GI₅₀ values ranging from 0.013 to >50 μ M and 0.003 to >50 μ M, respectively. Because many clinically used anticancer agents induce apoptosis in cancer cells, the compounds **6t** ($R = 3\text{-Br-4-OH-5-MeOC}_6\text{H}_2$) and **6u** ($R = 3\text{-Br-4,5-(MeO)}_2\text{C}_6\text{H}_2$) were tested for their ability to induce apoptosis in Jurkat (model for human T-cell leukemia) cells using a flow cytometric annexin-V/propidium iodide assay. Although compound **6t** is a strong apoptosis inducer at 100 nM, its potency drops as the concentration is reduced to 10 nM. In contrast, compound **6u** retains its potency at this low concentration. Moreover, the flow cytometric cell cycle analysis was performed with compounds **6t** and **6u** against the Jurkat cell line, showing a pronounced cell cycle arrest in the G₂/M phase (Table 4). Lastly, the effect of compounds **6t** and **6u** on *in vitro* tubulin polymerization was performed to support the proposed antitubulin mechanism of action. In this assay, the microtubule formation is monitored by the increase in fluorescence intensity of the reaction mixture. Paclitaxel exhibited a potent enhancement of the microtubule formation relative to the effect of DMSO control. In contrast, compounds **6t** and **6u** displayed a potent microtubule destabilizing effect like the known tubulin polymerization inhibitor Podophyllotoxin.

Importantly, a series of 4,6-diaryl-2-oxo-1,2-dihydropyridine-3-carbonitriles **9a–o** were synthesized through a four-

component reaction of various (hetero)aromatic aldehydes **1**, substituted acetophenones **7**, ethyl cyanoacetate **8**, and an excess of ammonium acetate in refluxing ethanol for 10 to 12 h (Scheme 1).⁴⁴ The precipitate obtained was subjected either to re-crystallization from a mixture of DMF/EtOH (1 : 10, v/v), or to column chromatography on silica gel to afford products **9a–o** in 62–92% yields. All compounds were evaluated for their *in vitro* anticancer activity against the human colon adenocarcinoma cell line HT29 using the MTT method. However, only the compounds **9b** ($R = 3\text{-ClC}_6\text{H}_4$, $R^1 = \text{C}_6\text{H}_5$) and **9d** ($R = 2\text{-EtOC}_6\text{H}_4$, $R^1 = 3\text{-thiophenyl}$) showed a significant anticancer activity with IC₅₀ values of 2.1 and 1.2 μ M, respectively.

Later, a molecular docking simulation was performed to investigate the interactions of compound **9d** with Pim-1 kinase (PDB ID code: 2OBJ) (Fig. 3). It was found that the oxygen atom of the carbonyl group and NH moiety form two hydrogen bonds with Lys67. Moreover, the nitrogen atom of the cyano group forms a hydrogen bond with Ser189, while the oxygen atom of the ethoxy group is involved in extra hydrogen bonding through a water molecule with Asp167, Asp186, and Ser189 residues.

To date, few reports are available in the literature regarding the eco-friendly synthesis of chromene-containing 2(1*H*)-pyridones. In this regard, the solventless synthesis of 4-aryl-6-[benzo[f]coumarin-3-yl]-3-cyano-2(1*H*)-pyridones **11a–d** was developed through a four-component reaction of aromatic aldehydes **1**, malononitrile **2**, and acetyl-3*H*-benzo[f]chromen-3-one **10** in the presence of sodium hydroxide at 75 °C for 45 min (Table 5).⁴⁵ Later, the reaction mixture was poured into water, and then washed with water, filtered, dried, and recrystallized from EtOH to furnish products **11a–d** in 71–87% yields. Some highlights of this protocol were associated with the absence of solvent, shorter reaction time, and a simple workup procedure. Lastly, 2(1*H*)-pyridone derivatives **11a–c** were evaluated for their *in vitro* anticancer activity against liver HepG2 and breast MCF-7 cell lines using the MTT method in the presence of 5-fluorouracil as a reference drug. In summary, compounds **11a–c**

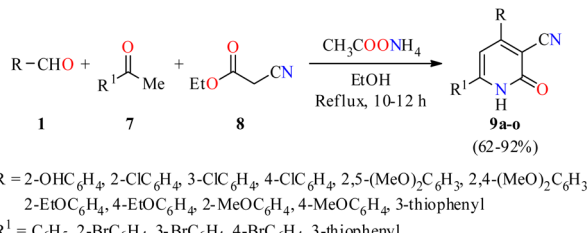
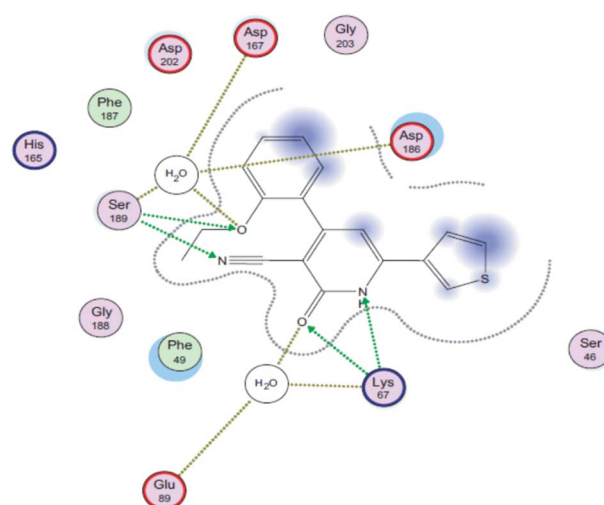
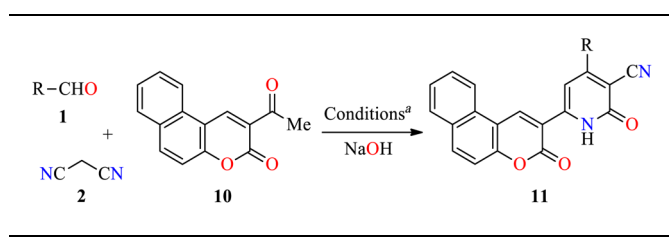
Scheme 1 Four-component synthesis and anticancer evaluation of 4,6-diaryl-2-oxo-1,2-dihydropyridine-3-carbonitriles **9**.Fig. 3 2D interactions of compound **9d** with Pim-1 kinase (PDB ID code: 2OBJ). Reproduced with permission from ref. 44. Copyright Elsevier Inc., 2022.

Table 5 Four-component synthesis and anticancer evaluation of chromene-based 2(1*H*)-pyridones 11



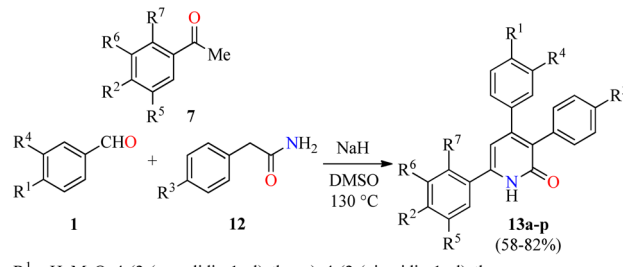
Compound	R	Yield 11 (%)	IC ₅₀ ^c (μM)	
			HePG2	MCF-7
11a	C ₆ H ₅	87	77.6	78.3
11b	4-OH C ₆ H ₄	85	58.1	59.9
11c	4-MeOC ₆ H ₄	79	53.6	56.3
11d	4-Me ₂ NC ₆ H ₄	71	—	—
5-Fluorouracil ^b	—	—	9.30	13.1

^a Reaction conditions: aldehyde 1 (1 mmol), malononitrile 2 (1.5 mmol), 2-acetyl-3H-benzof[*β*]chromen-3-one 10 (1 mmol), NaOH (1.5 mmol), 75 °C, 45 min. ^b Standard drug for the study. ^c Compound concentration required to reduce HePG2 and MCF-7 cells viability by 50% after 48 h treatment relative to 100% DMSO control as assessed with the MTT assay.

displayed a moderate cytotoxic effect with IC₅₀ values in the range of 53.6–77.6 μM and 56.3–78.3 μM for HepG2 and MCF-7 cell lines, respectively, when compared to 5-fluorouracil (IC₅₀ = 9.30 and 13.1 μM, respectively).

Importantly, the presence of electron donating groups such as hydroxy or methoxy substituents attached to the aromatic ring play an important role in the molecular interactions and have a profound effect on antiproliferative activity. In this regard, 3,4,6-triaryl-2(1*H*)-pyridones 13a–p were synthesized in 58–82% yields through a one-pot three-component reaction of aromatic aldehydes 1, substituted acetophenones 7, and phenyl acetamides 12 in the presence of sodium hydride in DMSO at 130 °C (Scheme 2).⁴⁶ All synthesized compounds 13a–p were evaluated for their *in vitro* anticancer activity against MCF-7 and MDA-MB-231 breast cancer cell lines using the MTT method in the presence of Nolvadex (tamoxifen citrate) as a standard drug. Data shown are average ± SD of two independent experiments. Remarkably, compound 13p (R¹ = 4-(2-(piperidin-1-yl)ethoxy, (R² = R³ = MeO, R⁴ = R⁵ = R⁶ = R⁷ = H) showed the most significant cytotoxic activity against MCF-7 and MDA-MB-231 cell lines with IC₅₀ values of 35.7 ± 5.8 μM and 16.8 ± 2.3 μM, respectively, when compared to Nolvadex (IC₅₀ = 8.8 ± 1.2 μM and 9.0 ± 1.3 μM, respectively). Cell cycle analysis showed that compound 13p induced arrest of cells in the G₁-phase and reduction in the S-phase cells in a dose-dependent manner. Moreover, compound 13p decreased ROS generation in a dose-dependent manner and induced ROS-independent mitochondrial-mediated apoptosis in MDA-MB-231 cells. Lastly, the apoptotic activity of compound 13p was also confirmed by DNA fragmentation and by expression of proapoptotic genes such as BAD, BAK, and BimL.

1,3-Dipolar cycloaddition reaction is one of the efficient ways for the regio- and stereoselective construction of five-membered



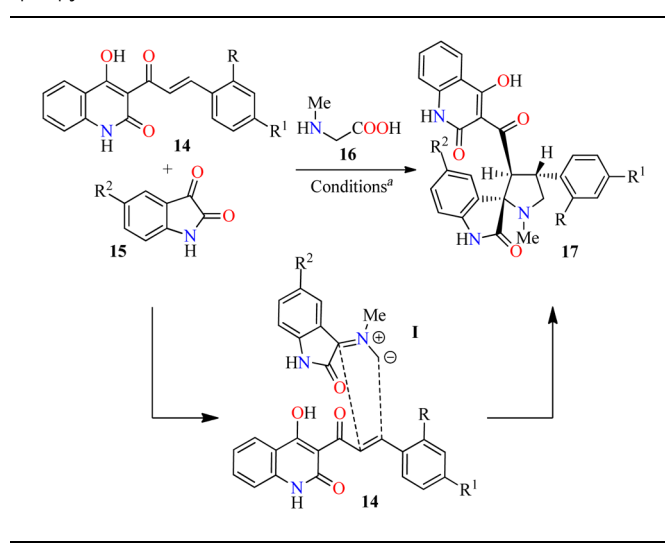
Scheme 2 One-pot three-component synthesis and anticancer evaluation of 3,4,6-triaryl-2(1*H*)-pyridones 13.

heterocycles.⁴⁷ In this sense, regioselective three-component synthesis of 4-hydroxyquinolin-2(1*H*)-one grafted spirocyclic ylides 17 has been accomplished through a 1,3-dipolar cycloaddition reaction of various azomethine ylides derived from isatin derivatives 15 and sarcosine 16 with 4-hydroxyquinolin-2(1*H*)-ones 14 as dipolarophile using a mixture of MeOH/H₂O (2 : 1, v/v) at reflux for 2.5–3.0 h (Table 6).⁴⁸ The reaction mixture was cooled at room temperature, and the products were filtered and recrystallized in a mixture of MeOH/DMF (7 : 3, v/v) to afford products 17a–g in 46–92% yields. Although the detailed mechanism of the reaction is not fully established, the regioselective formation of spirocyclic ylides 17 could involve a decarboxylative condensation of isatins 15 with sarcosine 16 to give azomethine ylides I, which undergo a 1,3-dipolar cycloaddition reaction with dipolarophiles 14. The regioselectivity in the product formation could be explained by considering the secondary orbital interaction (SOI) between the orbital of the carbonyl group of dipolarophiles 14 and those of azomethine ylides I. Moreover, the regio- and stereochemical outcome of the 1,3-dipolar cycloaddition reaction is ascertained by X-ray crystallography and spectroscopic techniques. The compounds 17 were screened for their *in vitro* anticancer activity against HCT-116 (colon cancer) and HeLa (cervical cancer) cell lines using the MTT method in the presence of Doxorubicin as a standard drug. Data shown are average ± SD of two independent experiments. Overall, compounds 17d (R = R¹ = H, R² = NO₂) and 17c (R = R² = H, R¹ = Me) showed the best anticancer activity against the HCT-116 cell line with IC₅₀ values of 9.3 and 9.6 μM, respectively, when compared to doxorubicin (IC₅₀ = 2.4 μM). Furthermore, compound 17b (R = Cl, R¹ = R² = H) showed a good anticancer activity against the HeLa cell line with an IC₅₀ value of 10.7 μM, in comparison to Doxorubicin (IC₅₀ = 1.8 μM).

Alternatively, Tangella and co-workers described the regio- and diastereoselective synthesis of *trans*-1,2-dihydrobenzofuro[3,2-*c*]quinolinones 20 in 77–90% yields via a three-component reaction of (hetero)aromatic aldehydes 1, α -bromoacetophenones 18, and 4-hydroxybenzo[*h*]quinolin-2(1*H*)-ones 19 in pyridine at 100 °C for 6 h (Scheme 3A).⁴⁹ The yields were found to be higher in case of substrates with electron-donating groups (*i.e.* R = 3,4,5-(MeO)₃C₆H₂, R¹ = 4-MeOC₆H₄, 90%) compared to substrates with electron-withdrawing groups (*i.e.* R = 4-NO₂C₆H₄, R¹ = C₆H₅, 77%). Moreover, heteroaryl aldehydes (R



Table 6 Three-component synthesis and anticancer evaluation of spiropyrrolidine derivatives **17**



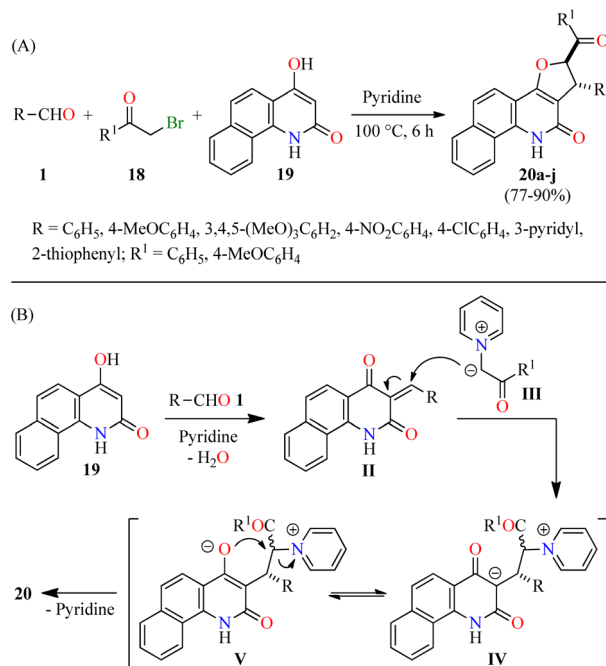
Compound	R	R ¹	R ²	Yield 17 (%)	HCT-116	HeLa	IC ₅₀ ^c (μM)
17a	H	H	H	92	83.2 ± 0.42	15.1 ± 0.18	
17b	Cl	H	H	88	—	10.7 ± 0.15	
17c	H	Me	H	62	9.6 ± 0.14	28.4 ± 0.30	
17d	H	H	NO ₂	54	9.3 ± 0.12	16.7 ± 0.14	
17e	H	Me	NO ₂	46	10.9 ± 0.18	25.5 ± 0.28	
17f	H	Cl	H	87	12.0 ± 0.20	34.6 ± 0.17	
17g	H	Br	H	82	—	—	
Doxorubicin ^b	—	—	—	—	2.4 ± 0.10	1.8 ± 0.05	

^a Reaction conditions: 4-hydroxyquinoline **14** (1.5 mmol), isatine **15** (1.5 mmol), sarcosine **16** (1.5 mmol), MeOH/H₂O (2 : 1, v/v), reflux, 2.5–3.0 h.

^b Standard drug for the study. ^c Compound concentration required to reduce HCT-116 and HeLa cells viability by 50% after 48 h treatment relative to 100% DMSO control as assessed with the MTT assay. Data shown are average ± SD of two independent experiments.

= 3-pyridyl and 2-thiophenyl) were found to be well tolerated and the corresponding products **20h–j** were obtained in 81–87% yields. The plausible reaction mechanism is briefly outlined in Scheme 3B.⁴⁹ The first step involves the formation of arylidenebenzo[*h*]quinoline-2,4-diones **II** through a pyridine-catalyzed Knoevenagel condensation of aldehydes **1** with 4-hydroxycoumarin derivatives **19**. The second step proceeds *via* a Michael addition of pyridinium ylides **III** with Knoevenagel adducts **II** to afford keto tautomers **IV**, which are in tautomeric equilibrium with enol tautomers **V**. Lastly, intermediates **V** undergo a diastereoselective intramolecular cyclization to give desired products **20**. Importantly, this protocol selectively generated *trans*-2,3-dihydrofuran derivatives due to the steric hindrance of the large substituents at C-2 (aryl) and C-3 (aryl or hetaryl), which are opposing one another in the transition state and the carbanion intermediate. In addition, pyridine plays different roles such as base, solvent, and a source of pyridinium ylides.

All compounds **20a–j** were evaluated for their *in vitro* cytotoxic activity against A549 (lung cancer), DU-145 (prostate

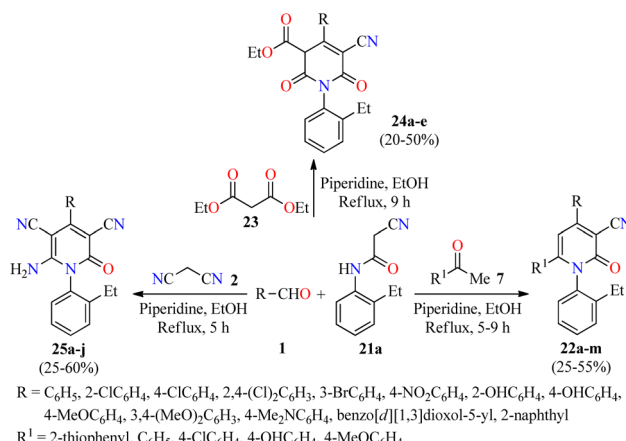


Scheme 3 (A) Three-component synthesis and anticancer evaluation of *trans*-2,3-dihydrofuran derivatives **20**. (B) Plausible reaction mechanism for the formation of **20**.

cancer), HeLa (cervical cancer), MCF-7 (breast cancer), and normal mouse fibroblast (NIH 3T3) cell lines using the MTT colorimetric assay in the presence of Doxorubicin as a standard drug.⁴⁹ The screening results revealed that all synthesized compounds showed selective cytotoxicity to cancer cells (IC₅₀ values ranging from 2.14 to 17.94 μM) with a very weak effect on normal cells (IC₅₀ values ranging from 70.43 to >100 μM). Most of the compounds showed prominent activity against the MCF-7 cell line compared to other tested cancer cell lines. In particular, compounds **20c** (R = R¹ = 4-MeOC₆H₄) and **20i** (R = 2-thiophenyl, R¹ = 4-MeOC₆H₄) displayed the best anticancer activity against the MCF-7 cell line with IC₅₀ values of 2.56 and 2.14 μM, respectively, when compared to Doxorubicin (IC₅₀ = 1.43 μM). Also, compound **20c** displayed high activity against A549 and DU-145 cell lines with IC₅₀ values of 6.05 and 3.28 μM, respectively, in comparison to Doxorubicin (IC₅₀ = 1.21 and 2.14 μM, respectively). In addition, compounds **20d** (R = 3,4,5-(MeO)₃C₆H₂, R¹ = C₆H₅) and **20f** (R = 4-NO₂C₆H₄, R¹ = C₆H₅) exerted significant activity against the HeLa cell line with IC₅₀ values of 4.89 and 4.35 μM, respectively (IC₅₀ = 1.63 μM for Doxorubicin).

A literature survey revealed that 4,6-diaryl-3-cyano-2-pyridones displayed a potent anticancer activity by inhibition of the Pim-1 kinase.^{50–52} In this regard, a novel series of substituted *N*-(2-ethylphenyl)-2-oxo-pyridine-3-carbonitriles **22** were synthesized in 25–55% yields through a piperidine-catalyzed three-component reaction of aromatic aldehydes **1**, substituted acetophenones **7**, and 2-cyano-*N*-(2-ethylphenyl)acetamide **21a** in refluxing ethanol for 5–9 h (Scheme 4).⁵³ This multicomponent protocol was extended to active methylene





Scheme 4 Three-component synthesis and anticancer evaluation of highly substituted 2-pyridone derivatives 22, 24, and 25.

Table 7 Flow cytometric cell cycle analysis of OVCAR-3 cell line

Compound	% Relative DNA content ^a		
	G ₀ /G ₁	S	G ₂ /M
DMSO	56.28	31.42	12.30
25g (4.09 μ M)	38.44	26.43	35.13
5-FU (10 μ M)	33.94	31.29	34.77

^a % Relative DNA content after 24 h treatment of OVCAR-3 cell line with indicated compounds.

compounds such as diethyl malonate 23 and malononitrile 2 to afford fully substituted 2-pyridone derivatives 24 and 25, respectively, in moderate yields. The anticancer activity of synthesized compounds was evaluated by the National Cancer Institute (NCI), which selected 14 compounds for one-dose screening. Among them, compound 25g ($R = 3,4-(MeO)_2C_6H_3$) was selected for five-dose screening, which displayed a potent anticancer activity with GI_{50} values ranging from 3.15 to 4.09 μ M against leukemia, CNS, colon, and ovarian cancer cell panels, and moderate cytotoxicity against the other cancer cell lines using the MTT method. Interestingly, cell cycle analysis against the OVCAR-3 (ovarian cancer) cell line showed that compound 25g induced apoptosis and arrested the cell cycle at the G₂/M phase, which was accompanied by a reduction in the S-phase cells (Table 7).

On the other hand, the provirus integration in Maloney (Pim) kinases are attractive drug targets because they are involved in cancer-specific pathways and upregulated in different hematological and solid cancers.⁵⁴ Among them, Pim-1 kinase has a significant role in the regulation of the cell cycle through phosphorylation of Cdc25 phosphatases and cell cycle inhibitors.⁵⁴ As a result, compound 25g was screened against Pim-1, Pim-2, and Pim-3 kinases using quercetin as a reference drug.⁵³ The results revealed more selectivity towards Pim-1 kinase ($IC_{50} = 1.89 \mu$ M) with a percentage inhibition of 64.6%, when compared to Quercetin ($IC_{50} = 1.22 \mu$ M). Lastly, molecular docking studies were performed to investigate the

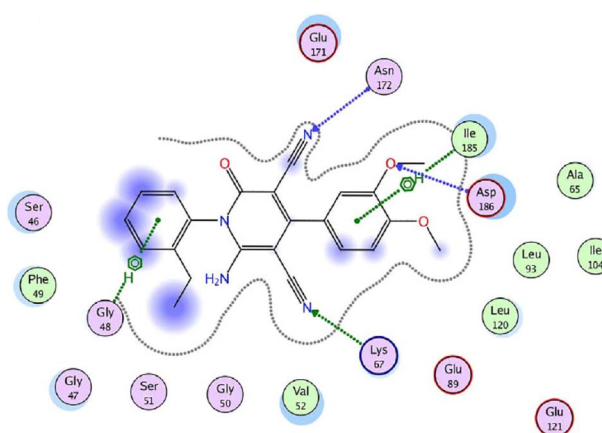
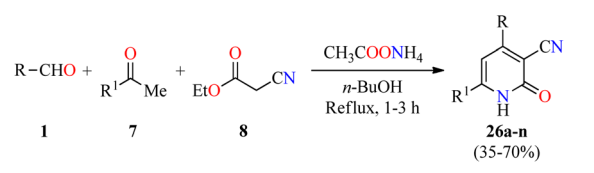


Fig. 4 2D interactions of compound 25g with Pim-1 kinase (PDB ID code: 2OBJ). Reproduced with permission from ref. 53. Copyright John Wiley & Sons Inc., 2022.

interactions of compound 25g with Pim-1 kinase (PDB ID code: 2OBJ) (Fig. 4). The nitrogen atom of cyano groups in positions 3 and 5 forms two hydrogen bonds with Asn172 and Lys67, respectively. Also, the oxygen atom of the methoxy group in position 3 forms a hydrogen bond with Asp186. Besides, 4-phenyl and 2-ethyl phenyl rings interact with Ile185 and Gly48 through an arene-H bonding, respectively.

Recently, a series of 4,6-diaryl-3-cyano-2(1*H*)-pyridones 26a-n were synthesized through a four-component reaction of various (hetero)aromatic aldehydes 1, substituted acetophenones 7, ethyl cyanoacetate 8, and an excess of ammonium acetate in refluxing *n*-butanol for 1–3 h (Scheme 5).⁵⁵ The precipitate was filtered, dried, and recrystallized from the appropriate solvent such as EtOH, AcOH, DMF, EtOH/AcOH (1 : 1, v/v), and DMF/AcOH (1 : 1, v/v) to afford products 26a-n in 35–70% yields. Selected compounds were screened for their *in vitro* anticancer activity against HepG2 (liver cancer) and THLE2 (normal liver cells) using the MTT assay in the presence of 5-fluorouracil as a reference drug. Data are expressed as mean \pm SD of three independent experiments. Interestingly, the compound 26n ($R = 4$ -MeOC₆H₄, $R^1 = 3$ -H₂NC₆H₄) showed good activity against HepG2 and THLE2 cells with IC_{50} values of $19.2 \pm 1.01 \mu$ M and $44.11 \pm 0.89 \mu$ M, respectively, in comparison to 5-fluorouracil ($IC_{50} = 6.98 \mu$ M for HepG2 cancer cell line). Moreover, the compound 26l ($R = 3$ -ClC₆H₄, $R^1 = 4$ -ClC₆H₄) displayed a moderate activity against HepG2 and THLE2 cells with IC_{50} values of $43.7 \pm 1.23 \mu$ M and $48.2 \pm 0.98 \mu$ M, respectively. Overall, tested compounds



Scheme 5 Four-component synthesis and anticancer evaluation of 2(1*H*)-pyridone derivatives 26.

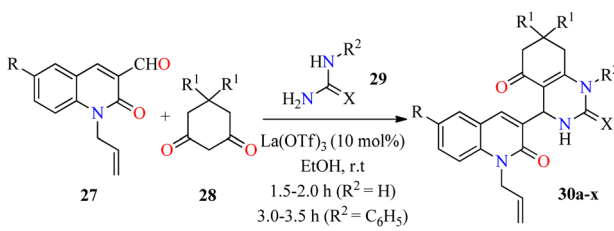


were safe against normal liver cells with IC_{50} values ranging from 44.1 to $\geq 50 \mu\text{M}$.

2.2. Antibacterial activity

Over the past few decades antibacterial drugs (*i.e.* Amphotericin B, Fluconazole, Penicillin, Chloramphenicol, among others) become less effective or even ineffective due to their emerging antimicrobial resistance. In regards to this case, innovative synthetic strategies will be required to develop new molecules with potential antibacterial properties against a wide range of bacteria.^{56,57} In this regard, an efficient three-component reaction of 2-oxo-1,2-dihydroquinoline-3-carbaldehydes 27, cyclohexane-1,3-dione derivatives 28, and (thio)urea 29a ($R^2 = \text{H}$) catalyzed by $\text{La}(\text{OTf})_3$ (10 mol%) in ethanol at room temperature for 1.5–2.0 h afforded *N*-allylquinolone derivatives 30a–p (Scheme 6).⁵⁸ This multicomponent approach was successfully extended to *N*-phenylthiourea 29b ($R^2 = \text{C}_6\text{H}_5$) under similar reaction conditions for 3.0–3.5 h to give *N*-allylquinolone derivatives 30q–x. After the completion of the reaction, the solid was filtered, washed with ethanol, and purified by leaching in an equal volume ratio of chloroform and methanol to obtain products 30 in good yields. Subsequently, compounds 30a–x were screened against Gram-negative (*Escherichia coli* and *Pseudomonas aeruginosa*) and Gram-positive (*Staphylococcus aureus* and *Streptococcus pyogenes*) bacterial strains by using the agar well diffusion method in the presence of ciprofloxacin as a standard drug. Interestingly, the compound 30h ($R = R^1 = \text{Me}$, $R^2 = \text{H}$, $X = \text{S}$) showed the highest activity against *Pseudomonas aeruginosa* with a MIC value of $20 \mu\text{g mL}^{-1}$, while compounds 30r ($R = \text{H}$, $R^1 = \text{Me}$, $R^2 = \text{C}_6\text{H}_5$, $X = \text{S}$) and 30x ($R = \text{Cl}$, $R^1 = \text{Me}$, $R^2 = \text{C}_6\text{H}_5$, $X = \text{S}$) were the most active against *Escherichia coli* with a MIC value of $50 \mu\text{g mL}^{-1}$, in comparison to Ciprofloxacin (MIC = $25 \mu\text{g mL}^{-1}$ for both strains). Moreover, compounds 30f ($R = R^1 = \text{Me}$, $R^2 = \text{H}$, $X = \text{O}$) and 30w ($R = \text{Cl}$, $R^1 = \text{H}$, $R^2 = \text{C}_6\text{H}_5$, $X = \text{S}$) displayed a good activity against *Staphylococcus aureus* with a MIC value of $62.5 \mu\text{g mL}^{-1}$, when compared to ciprofloxacin (MIC = $50 \mu\text{g mL}^{-1}$). Lastly, compounds 30e ($R = \text{Me}$, $R^1 = R^2 = \text{H}$, $X = \text{O}$), 30g ($R = \text{Me}$, $R^1 = R^2 = \text{H}$, $X = \text{S}$), 30m ($R = \text{Cl}$, $R^1 = R^2 = \text{H}$, $X = \text{O}$), and 30p ($R = \text{Cl}$, $R^1 = \text{Me}$, $R^2 = \text{H}$, $X = \text{S}$) exerted a moderate MIC value of $100 \mu\text{g mL}^{-1}$ against *Streptococcus pyogenes*, in comparison to Ciprofloxacin (MIC = $50 \mu\text{g mL}^{-1}$).

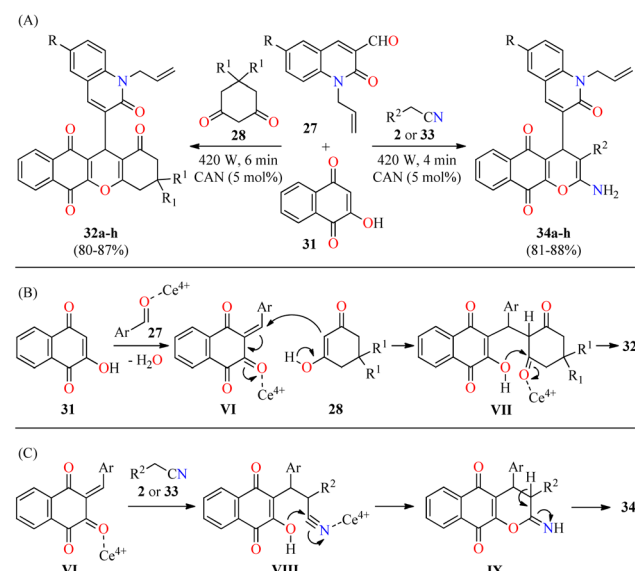
In a similar way to previously mentioned,⁵⁸ the same authors reported the solventless synthesis of *N*-allylquinolone



Scheme 6 $\text{La}(\text{OTf})_3$ -catalyzed three-component synthesis and antibacterial evaluation of *N*-allylquinolone derivatives 30.

derivatives 32 in 80–87% yields through a solventless three-component reaction of *N*-allyl quinolone-3-carbaldehydes 27, cyclohexane-1,3-dione derivatives 28, and 2-hydroxy-1,4-naphthoquinone 31 catalyzed by ceric ammonium nitrate (5 mol%) in a microwave oven at 420 W for 6 min (Scheme 7A).⁵⁹ This multicomponent approach was successfully extended to malononitrile/*iso*-propylcyanoacetate 2/33 under similar reaction conditions at 420 W for 4 min to give *N*-allylquinolone derivatives 34 in 81–88% yields. This methodology was distinguished by its high yields, short reaction times, and solvent-free conditions. The plausible mechanistic pathways for products 32 and 34 are illustrated in Scheme 7B and C, respectively. It was supposed that the reaction occurred *via* the *ortho*-quinone methides VI, which are formed by the nucleophilic addition of 2-hydroxy-1,4-naphthoquinone 31 to quinolone-3-carbaldehydes 27 catalyzed with CAN. Subsequent attack of cyclic 1,3-dicarbonyl compounds 28 (enol form) to the *ortho*-quinone methides VI gives intermediates VII, which undergo 6-*exo-trig* intramolecular cyclization/elimination sequence to afford compounds 32. Alternatively, the Michael addition of malononitrile/*iso*-propylcyanoacetate 2/33 to the *ortho*-quinone methides VI gives intermediates VIII, which undergo 6-*exo-dig* intramolecular cyclization/tautomerization sequence to furnish compounds 34. The rapid formation of compounds 34 may be due to the nucleophilic attack of the hydroxy group on the highly electrophilic carbon atom of the nitrile group (VIII) compared to the carbon atom of the carbonyl group (VII).

The compounds 32a–h and 34a–h were screened for their antibacterial activity against two Gram-positive (*Staphylococcus aureus* and *Streptococcus pyogenes*) and two Gram-negative (*Escherichia coli* and *Pseudomonas aeruginosa*) bacterial strains using Ciprofloxacin as a standard drug. The compounds 32 and



Scheme 7 (A) CAN-catalyzed three-component synthesis of *N*-allylquinolone derivatives 32 and 34 and their *in vitro* antibacterial activity against four bacterial strains. (B) Plausible reaction mechanism for the formation of 32. (C) Plausible reaction mechanism for the formation of 34.



34 showed moderate to excellent antibacterial activity with MIC values in the range of 20 to 500 $\mu\text{g mL}^{-1}$, in comparison to Ciprofloxacin (MIC = 25–50 $\mu\text{g mL}^{-1}$). In particular, compounds **34a** (R = H, R² = CN) and **32d** (R = Cl, R¹ = H) showed the highest activity against *Staphylococcus aureus* and *Streptococcus pyogenes* with MIC values of 62.5 and 50 $\mu\text{g mL}^{-1}$, respectively. Remarkably, compounds **34f** (R = Me, R² = COO-*i*-Pr) and **32c** (R = MeO, R¹ = H) displayed an excellent potency against *Escherichia coli* and *Pseudomonas aeruginosa* with MIC values of 25 and 20 $\mu\text{g mL}^{-1}$, respectively, which are equipotent to Ciprofloxacin (MIC = 25 $\mu\text{g mL}^{-1}$ for both strains).

The 4-aryl-6-[benzo[f]coumarin-3-yl]-3-cyano-2(1*H*)-pyridones **11a–d** obtained by a four-component process and discussed in Section 2.1. Anticancer activity (Table 5),⁴⁵ were also screened for their antibacterial activity against two Gram-positive (*Bacillus subtilis* and *Enterococcus faecalis*) and one Gram-negative (*Salmonella typhimurium*) bacterial strains by using the disk diffusion method in the presence of Ampicillin and Chloramphenicol as standard drugs (Table 8). The compounds showed a diameter of growth of inhibition zone in the range of 10–13 mm, 9–11 mm, and 8–12 mm against *Bacillus subtilis*, *Enterococcus faecalis*, and *Salmonella typhimurium*, respectively, in comparison to Ampicillin (13–25 mm) and Chloramphenicol (18–24 mm). Overall, the Gram-negative bacterium was more susceptible to the synthesized compounds than Gram-positive bacteria. Remarkably, compounds **11d** (R = 4-Me₂NC₆H₄) and **11c** (R = 4-MeOC₆H₄) showed the highest activity against *Salmonella typhimurium* with a diameter of growth of inhibition zone of 11 and 12 mm, respectively, when compared to Ampicillin (13 mm) and Chloramphenicol (18 mm).

Interestingly, a series of coumarin–pyridone hybrids **37** were obtained in 79–93% yields through a one-pot three-component reaction of (*E*)-3-(3-arylacryloyl)-2*H*-chromen-2-ones **35**, ethyl 2-nitroacetate **36**, and an excess of ammonium acetate in refluxing

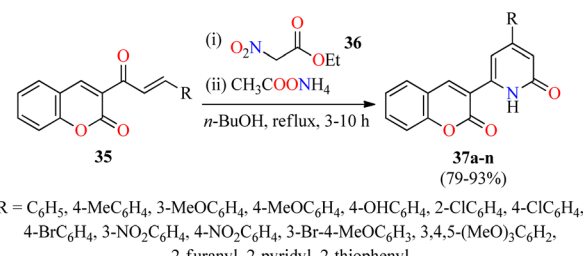
Table 8 Four-component synthesis of chromene-based 2(1*H*)-pyridones **11** and their *in vitro* antibacterial activity against three bacterial strains^a

Compound	R	Inhibition zone (mm)		
		BS	EF	ST
11a	C ₆ H ₅	12	11	—
11b	4-OHC ₆ H ₄	13	9	8
11c	4-MeOC ₆ H ₄	12	10	12
11d	4-Me ₂ NC ₆ H ₄	10	10	11
Ampicillin ^b	—	25	20	13
Chloramphenicol ^b	—	24	23	18

^a BS (*Bacillus subtilis*), EF (*Enterococcus faecalis*), ST (*Salmonella typhimurium*). ^b Standard drug for the study.

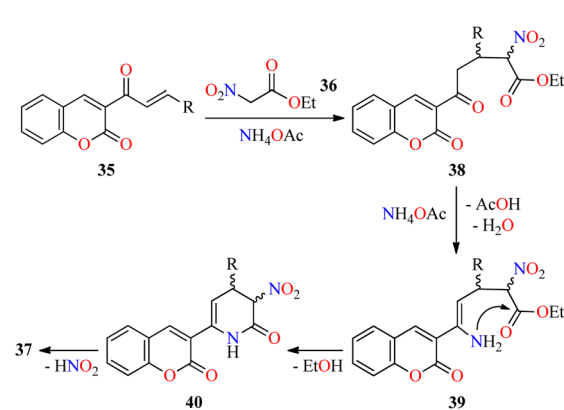
n-BuOH for 3–10 h (Scheme 8).⁶⁰ The reaction mixture was cooled to room temperature and the precipitate was filtered, washed, and recrystallized from EtOH to obtain the product **37**. This approach shows a broad substrate scope and excellent functional-group tolerance with diverse electron-rich and electron-deficient substituents. A plausible mechanism proposed by the authors is shown in Scheme 9. Initially, α,β -unsaturated ketones **35** reacted with ethyl 2-nitroacetate **36** through a Michael addition/condensation sequence mediated by ammonium acetate to give enamine-type intermediates **39**, which subsequently underwent an intramolecular cyclization to generate 3,4-dihydropyridin-2(1*H*)-ones **40**. Lastly, the elimination of HNO₂ afforded coumarin–pyridone hybrids **37**. The compounds **37a–n** were screened for their antibacterial activity against three Gram-positive (*Bacillus subtilis*, *Klebsiella pneumoniae*, and *Staphylococcus aureus*) and two Gram-negative (*Escherichia coli* and *Pseudomonas aeruginosa*) bacterial strains using Ciprofloxacin as a standard drug. It was found that compounds **37d** (R = 4-MeOC₆H₄), **37i** (R = 3-NO₂C₆H₄), **37k** (R = 3-Br-4-MeOC₆H₃), and **37o** (R = 2-pyridyl) exhibited a moderate activity with MIC values in the range of 60–80 $\mu\text{g mL}^{-1}$, in comparison to Ciprofloxacin (MIC = 0.03–8.0 $\mu\text{g mL}^{-1}$).

Alternatively, Pandit and co-workers described the piperidine-catalyzed synthesis of fully substituted 2(1*H*)-pyridone derivatives **43** via a three-component reaction of (hetero) aromatic aldehydes **1**, acetoacetanilide **41**, and cyanoacetamide **42** in refluxing ethanol for 7–8 h (Scheme 10).⁶¹ The reaction

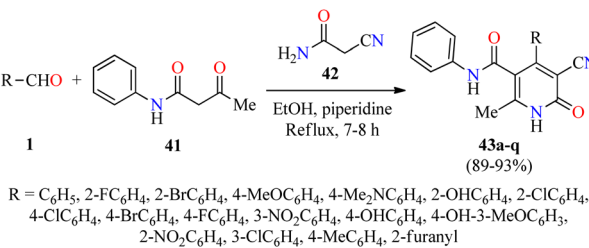


R = C₆H₅, 4-MeC₆H₄, 3-MeOC₆H₄, 4-MeOC₆H₄, 4-OHC₆H₄, 2-ClC₆H₄, 4-ClC₆H₄, 4-BrC₆H₄, 3-NO₂C₆H₄, 4-NO₂C₆H₄, 3-Br-4-MeOC₆H₃, 3,4,5-(MeO)₃C₆H₂, 2-furanyl, 2-pyridyl, 2-thiophenyl

Scheme 8 One-pot three-component synthesis of coumarin–pyridone hybrids **37** for evaluation of their antibacterial activity.



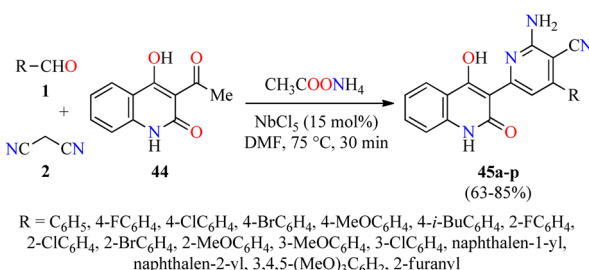
Scheme 9 Plausible mechanism for the synthesis of coumarin–pyridone hybrids **37**.



Scheme 10 Piperidine-catalyzed three-component synthesis of 2(1H)-pyridone derivatives **43** for evaluation of their antibacterial activity.

mixture was cooled in a refrigerator overnight and the precipitate was filtered, washed with EtOH, and dried to obtain the products **43** in 89–93% yields. Selected compounds were screened for their antibacterial activity against two Gram-positive (*Bacillus subtilis* and *Staphylococcus aureus*) and two Gram-negative (*Escherichia coli* and *Pseudomonas aeruginosa*) bacterial strains. Overall, the compounds **43c** (R = 2-BrC₆H₄) and **43q** (R = 2-furanyl) showed a diameter of growth of inhibition zone in the range of 3.50–4.25 mm and 1.50–3.75 mm for Gram-positive and Gram-negative bacterial strains, respectively.

Quinolone analogs have a broad spectrum of antimicrobial properties. For instance, Krishna and colleagues described the synthesis of quinolone–pyridine hybrids **45** in 63–85% yields through a time-efficient four-component reaction of (hetero)aromatic aldehydes **1**, malononitrile **2**, 3-acetyl-4-hydroxy-2(1H)-quinolone **44**, and an excess of ammonium acetate catalyzed by NbCl₅ (15 mol%) in DMF at 75 °C for 30 min (Scheme 11).⁶² The compounds **45a–p** were screened for their antibacterial activity against two Gram-positive (*Staphylococcus aureus* and *Bacillus cereus*) and three Gram-negative (*Klebsiella planticola*, *Escherichia coli*, and *Pseudomonas aeruginosa*) bacterial strains using Ciprofloxacin hydrochloride as a standard drug. It was found that compound **45e** (R = 4-MeOC₆H₄) exhibited an excellent activity against *Staphylococcus aureus* and *Bacillus cereus* with a MIC value of 2.34 µg mL⁻¹, in comparison to Ciprofloxacin hydrochloride (MIC = 4.68 and 2.34 µg mL⁻¹, respectively). In case of *Klebsiella planticola*, compounds **45c** (R = 4-ClC₆H₄), **45h** (R = 2-ClC₆H₄), and **45p** (R = 2-furanyl) showed the same activity than standard drug with a MIC value of 4.68 µg mL⁻¹. Lastly, compounds **45e** (R = 4-MeOC₆H₄), **45f** (R = 4-i-BuC₆H₄), and **45p** (R = 2-furanyl) exhibited higher antibacterial activity

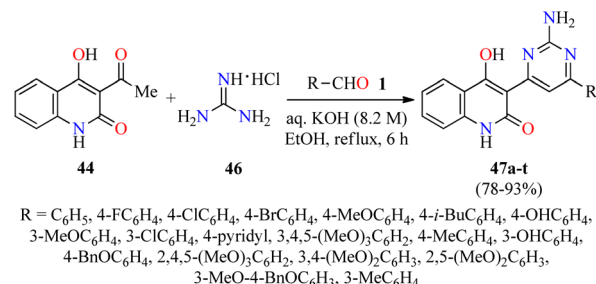


Scheme 11 NbCl₅-catalyzed four-component synthesis of quinolone–pyridine hybrids **45** for evaluation of their antibacterial activity.

than standard drug against *Escherichia coli* with a MIC value of 2.34 µg mL⁻¹, while the compound **45i** (R = 2-BrC₆H₄) displayed a good potency against *Pseudomonas aeruginosa* with a MIC value of 4.68 µg mL⁻¹, in comparison to Ciprofloxacin hydrochloride (MIC = 4.68 and 2.34 µg mL⁻¹, respectively).

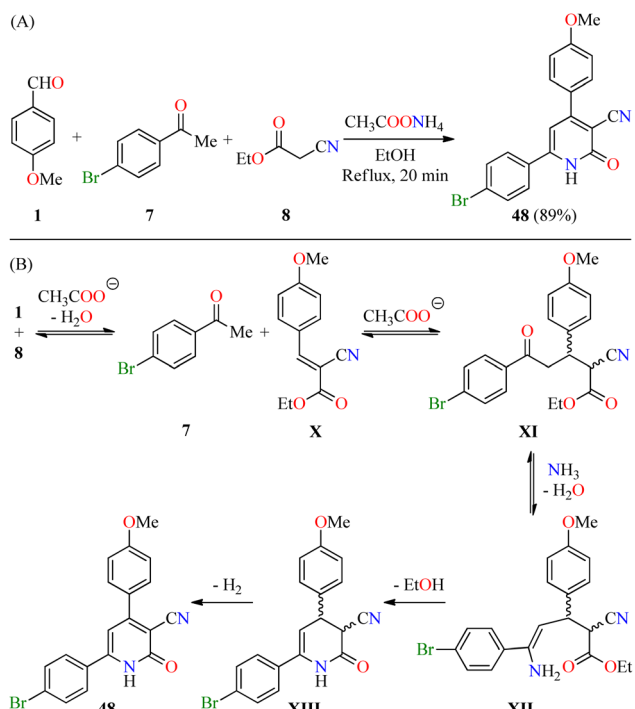
A year later, the same authors employed a similar strategy for the synthesis of quinolone–pyrimidine hybrids **47** by a three-component reaction of (hetero)aromatic aldehydes 1,3-acetyl-4-hydroxy-2(1H)-quinolone **44**, and an excess of guanidine hydrochloride **46** in an aqueous solution of KOH under refluxing ethanol for 6 h (Scheme 12).⁶³ Purification of products by column chromatography was unsuccessful due to their poor solubility. For that reason, the crude product was diluted with 100 mL of water and the pH was adjusted to 2.0 by using a hydrochloric acid solution (6.0 M). The resulting solid was filtered, washed with water, dried, and recrystallized in ethanol to give the products **47** in 78–93% yields. All synthesized compounds **47a–t** were screened for their antibacterial activity against two Gram-positive (*Staphylococcus aureus* and *Bacillus cereus*) and three Gram-negative (*Klebsiella planticola*, *Escherichia coli*, and *Pseudomonas aeruginosa*) bacterial strains using Neomycin as a standard drug. It was found that compound **47s** (R = 3-MeO-4-BnOC₆H₃) exhibited the highest activity against *Staphylococcus aureus*, while compounds **47k** (R = 3,4,5-(MeO)₃C₆H₂) and **47m** (R = 3-OHC₆H₄) showed the best activity against *Bacillus cereus* with a MIC value of 0.58 µg mL⁻¹ in both cases, when compared to Neomycin (MIC = 18.75 µg mL⁻¹ for both strains). In addition, compounds **47m** and **47r** (R = 2,5-(MeO)₂C₆H₃) resulted to be more potent than Neomycin against *Klebsiella planticola* and *Pseudomonas aeruginosa* with a MIC value of 0.58 µg mL⁻¹, respectively. The compounds **47c** (R = 4-ClC₆H₄), **47f** (R = 4-i-BuC₆H₄), **47k**, and **47n** (R = 4-BnOC₆H₄) showed an excellent antibacterial activity against *Escherichia coli* with a MIC value of 1.17 µg mL⁻¹, in comparison to Neomycin (MIC = 18.75 µg mL⁻¹).

Recently, El-Hashasha and co-workers described the time-efficient synthesis of 4,6-diaryl-3-cyano-2(1H)-pyridone **48** by a four-component reaction of 4-methoxybenzaldehyde **1**, 4-bromoacetophenone **7**, ethyl cyanoacetate **8**, and an excess of ammonium acetate in refluxing ethanol for 20 min (Scheme 13A).⁶⁴ The precipitate was filtered, dried, and recrystallized from methanol to afford product **48** in 89% yield. The plausible mechanism reaction proceeds *via* a Knoevenagel condensation



Scheme 12 Three-component synthesis of quinolone–pyrimidine hybrids **47** for evaluation of their antibacterial activity.

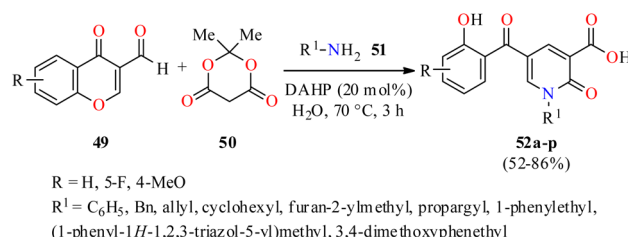




Scheme 13 (A) Four-component synthesis of the 4,6-diaryl-3-cyano-2(1H)-pyridone **48** and its *in vitro* antibacterial activity against two bacterial strains. (B) Plausible reaction mechanism for the formation of **48**.

of 4-methoxybenzaldehyde **1** with ethyl cyanoacetate **8** to afford cyanoacrylate **X**, which undergoes a Michael addition with 4-bromoacetophenone **7** to give intermediate **XI** (Scheme 13B). The condensation reaction of 1,5-dicarbonyl compound **XI** with ammonia gives enamine intermediate **XII**, which undergoes an intramolecular cyclization/dehydrogenation sequence to deliver the desired product **48**. Interestingly, the functionalization of compound **48** afforded pyridine and triazole derivatives in high yields. Lastly, compound **48** was screened for its antibacterial activity against *Staphylococcus aureus* and *Escherichia coli* as Gram-positive and Gram-negative bacterial strains, respectively, using Cefoxitin as a standard drug. It was found that compound **48** displayed a diameter of growth of the inhibition zone of 13 mm and 12 mm against *Staphylococcus aureus* and *Escherichia coli*, respectively, in comparison to Cefoxitin (25 mm for both strains).

Interestingly, 2-pyridone-3-carboxylic acids **52** were synthesized in 52–86% yields through a three-component reaction of 3-formylchromones **49**, Meldrum's acid **50**, and primary amines **51** in the presence of diammonium hydrogen phosphate (DAHP, 20 mol%) as a basic catalyst in water at 70 °C for 3 h (Scheme 14).⁶⁵ This protocol was distinguished by its operational simplicity, good yields, short reaction times, and structural diversity of products by the use of different aliphatic and aromatic amines. The compounds **52a–p** were screened for their antibacterial activity against two Gram-positive (*Staphylococcus aureus* and Methicillin-resistant *Staphylococcus aureus*) and two Gram-negative (*Escherichia coli* and *Acinetobacter baumannii*)



Scheme 14 DAHP-catalyzed three-component synthesis of 2-pyridone-3-carboxylic acids **52** and their *in vitro* antibacterial activity against four bacterial strains.

bacterial strains using Cefixime and Ciprofloxacin as standard drugs. It was found that compounds **52p** ($R = 4\text{-MeO}$, $R^1 = \text{cyclohexyl}$) and **52b** ($R = \text{H}$, $R^1 = \text{allyl}$) exhibited the highest activity against *Staphylococcus aureus* with MIC values of 2.96 and 4.67 $\mu\text{g mL}^{-1}$, respectively, in comparison to Cefixime ($\text{MIC} = 1 \mu\text{g mL}^{-1}$) and Ciprofloxacin ($\text{MIC} = 0.25 \mu\text{g mL}^{-1}$). In addition, the compound **52o** ($R = 4\text{-MeO}$, $R^1 = \text{allyl}$) showed the best activity against Methicillin-resistant *Staphylococcus aureus* with a MIC value of 82.33 $\mu\text{g mL}^{-1}$, when compared to Cefixime ($\text{MIC} = 32 \mu\text{g mL}^{-1}$) and Ciprofloxacin ($\text{MIC} = 64 \mu\text{g mL}^{-1}$). In case of *Escherichia coli*, the compound **52h** ($R = \text{H}$, $R^1 = 3,4\text{-dimethoxyphenethyl}$) showed a moderate activity with a MIC value of 12.79 $\mu\text{g mL}^{-1}$, while all synthesized compounds **52a–p** displayed a low antibacterial activity against *Acinetobacter baumannii* with MIC values ranging from 329.32 to $>500 \mu\text{g mL}^{-1}$, when compared to Cefixime ($\text{MIC} = 4$ and 32 $\mu\text{g mL}^{-1}$, respectively) and Ciprofloxacin ($\text{MIC} = 0.5$ and 64 $\mu\text{g mL}^{-1}$, respectively).

Lastly, molecular docking studies were performed to investigate the interactions of compound **52p** ($R = 4\text{-MeO}$, $R^1 = \text{cyclohexyl}$) with the DNA gyrase active site (PDB ID code: 5CDQ) (Fig. 5).⁶⁵ 2-Hydroxy-4-methoxybenzoyl interacted with Arg458 and Asp437 through π -cation and H-bonding, respectively. Also, *N*-cyclohexane and carbonyl groups occupied the proximity of Gly81 and formed H-bonding interaction with Ser84, respectively. Interestingly, the electron-donating property of the

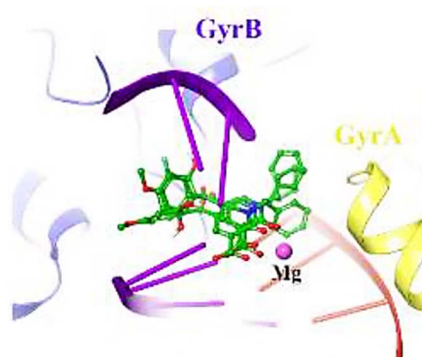


Fig. 5 3D Interactions of compound **52p** with *Staphylococcus aureus* DNA gyrase (PDB ID code: 5CDQ). GyrA and GyrB subunit of DNA gyrase are in yellow and blue, respectively.

methoxy substitution at the benzoyl ring increased the tendency of the compound **52p** to make π -cation interaction with Arg458.

2.3. Antifungal activity

For decades, fungal infections have been difficult health conditions to treat due to their high toxicity, low efficacy rates, long duration of treatment, and resistance to clinically anti-fungal drugs.⁶⁶ These reasons have prompted the development of new antifungal agents with distinct action or multitargeted combination therapy.^{66–68} In this way, *N*-allylquinolone derivatives **30** were obtained through a La(OTf)₃-catalyzed three-component reaction and discussed in Section 2.2. Antibacterial activity (Scheme 6).⁵⁸ The antifungal activity of these compounds was evaluated against *Candida albicans*, *Aspergillus niger*, and *Aspergillus clavatus* using Nystatin as a standard drug. Overall, *N*-allylquinolone derivatives **30** showed MIC values in the range of 100 to >1000 $\mu\text{g mL}^{-1}$ for three fungal strains, in comparison to Nystatin (MIC = 100 $\mu\text{g mL}^{-1}$ for all strains). Interestingly, the compound **30r** (R = H, R¹ = Me, R² = C₆H₅, X = S) showed a significant activity against *Candida albicans* with a MIC value of 200 $\mu\text{g mL}^{-1}$. Also, compounds **30w** (R = Cl, R¹ = H, R² = C₆H₅, X = S) and **30x** (R = Cl, R¹ = Me, R² = C₆H₅, X = S) displayed the same activity that Nystatin against *Aspergillus niger* and *Aspergillus clavatus*, respectively, with a MIC value of 100 $\mu\text{g mL}^{-1}$.

On the other hand, *N*-allylquinolone derivatives **32** and **34** obtained by a solvent-free microwave-assisted multicomponent process and discussed in Section 2.2. Antibacterial activity (Scheme 7),⁵⁹ were also screened for their antifungal activity against *Candida albicans*, *Aspergillus niger*, and *Aspergillus clavatus* using Nystatin as a standard drug. The compounds **32a** (R = R¹ = H) and **34a** (R = H, R² = CN) showed a moderate activity against *Candida albicans* with a MIC value of 250 $\mu\text{g mL}^{-1}$, in comparison to Nystatin (MIC = 100 $\mu\text{g mL}^{-1}$). Importantly, compounds **32c** (R = MeO, R¹ = H) and **34h** (R = Cl, R² = COO-*i*-Pr) exerted an excellent activity against *Aspergillus niger*, while the compounds **32d** (R = Cl, R¹ = H), **32h** (R = Cl, R¹ = Me), and **34d** (R = Cl, R² = CN) displayed the highest potency against *Aspergillus clavatus* with a MIC value of 100 $\mu\text{g mL}^{-1}$ in all cases, when compared to Nystatin (MIC = 100 $\mu\text{g mL}^{-1}$ for both strains).

Importantly, coumarin–pyridone hybrids **37** obtained through a one-pot three-component approach and discussed in Section 2.2. Antibacterial activity (Scheme 8),⁶⁰ were also screened for their antifungal activity against *Candida albicans*, *Aspergillus fumigatus*, and *Aspergillus niger* using Amphotericin B as a standard drug. It was found that compounds **37d** (R = 4-MeOC₆H₄) and **37m** (R = 2-furanyl) exhibited a moderate activity with MIC values in the range of 60–75 $\mu\text{g mL}^{-1}$ against three fungal strains, in comparison to Amphotericin B (MIC = 0.5–1.0 $\mu\text{g mL}^{-1}$, respectively).

Alternatively, fully substituted 2(1*H*)-pyridone derivatives **43** obtained by a piperidine-catalyzed three-component approach and discussed in Section 2.2. Antibacterial activity (Scheme 10),⁶¹ were also screened for their antifungal activity against *Aspergillus niger*. It was found that compounds **43a** (R = C₆H₅),

43b (R = 2-FC₆H₄), **43c** (R = 2-BrC₆H₄), **43d** (R = 4-MeOC₆H₄), **43e** (R = 4-Me₂NC₆H₄), and **43q** (R = 2-furanyl) showed a diameter of growth of inhibition zone in the range of 3.00–3.75 mm against *Aspergillus niger*. Unfortunately, the authors did not use a standard drug for this study.

Alternatively, Krishna and colleagues described the synthesis of quinolone–pyridine hybrids **45** via an NbCl₅-catalyzed four-component reaction and discussed in Section 2.2. Antibacterial activity (Scheme 11),⁶² were also screened for their antifungal activity against *Candida albicans*, *Candida parapsilosis*, *Candida glabrata*, *Candida aaseri*, *Aspergillus niger*, and *Issatchenka hanoiensis* using Miconazole as a standard drug. Particularly, the compound **45n** (R = naphthalene-2-yl) showed the highest activity against tested *Candida* and fungal pathogens with MIC values ranging from 1.67 to 9.37 $\mu\text{g mL}^{-1}$, in comparison to Miconazole (MIC = 4.68–9.37 $\mu\text{g mL}^{-1}$). Moreover, compounds **45b** (R = 4-FC₆H₄), **45d** (R = 4-BrC₆H₄), **45f** (R = 4-*i*-BuC₆H₄), **45n**, and **45p** (R = 2-furanyl) showed an excellent antifungal activity against *Candida* strains with MIC values in the range of 2.34–9.37 $\mu\text{g mL}^{-1}$, in comparison to Miconazole (MIC = 4.68–9.37 $\mu\text{g mL}^{-1}$). In cases of *Aspergillus niger* and *Issatchenka hanoiensis*, compounds **45a** (R = C₆H₅), **45d**, and **45n** displayed a high potency with MIC values in the range of 1.67–9.37 $\mu\text{g mL}^{-1}$, respectively, in comparison to Miconazole (MIC = 9.37 $\mu\text{g mL}^{-1}$).

A year later, the same authors used a similar strategy for the synthesis of quinolone–pyrimidine hybrids **47** by a three-component protocol as discussed in Section 2.2. Antibacterial activity (Scheme 12),⁶³ were also tested for their antifungal activity against *Candida albicans*, *Candida parapsilosis*, *Candida glabrata*, *Candida aaseri*, *Aspergillus niger*, and *Issatchenka hanoiensis* using Miconazole as a standard drug. Overall, compounds **47h** (R = 3-MeOC₆H₄), **47r** (R = 2,5-(MeO)₂C₆H₃), and **47t** (R = 3-MeC₆H₄) showed the highest antifungal activity against *Candida* strains with MIC values ranging from 0.58 to 1.17 $\mu\text{g mL}^{-1}$, in comparison to Miconazole (MIC = 4.68–9.37 $\mu\text{g mL}^{-1}$). In cases of *Aspergillus niger* and *Issatchenka hanoiensis*, compounds **47r** and **47n** (R = 4-BnOC₆H₄) exerted an excellent activity with a MIC value of 0.58 $\mu\text{g mL}^{-1}$, respectively, in comparison to Miconazole (MIC = 9.37 $\mu\text{g mL}^{-1}$).

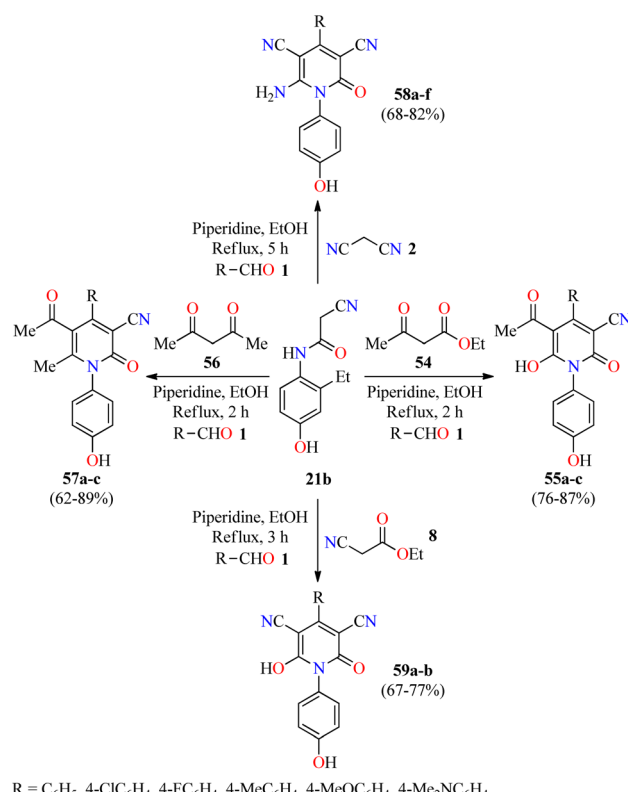
Lastly, 2-pyridone-3-carboxylic acids **52** obtained through a DAHP-catalyzed three-component approach and discussed in Section 2.2. Antibacterial activity (Scheme 14),⁶⁵ were also screened for their antifungal activity against *Candida albicans* using Nystatin as a standard drug. Unfortunately, all compounds **52a–p** exhibited a low antifungal activity with a MIC value of >500 $\mu\text{g mL}^{-1}$, in comparison to Nystatin (MIC = 64 $\mu\text{g mL}^{-1}$).

2.4. Anti-inflammatory activity

Inflammation is a self-protective procedure to eliminate the injurious stimuli and to start the healing process. Importantly, inflammation is a critical component of tumor progression.^{69,70} Thus, the anti-inflammatory therapy is efficacious towards early neoplastic progression and malignant conversion.^{69,70} Most of the commercially available anti-inflammatory drugs are found to be highly unsafe for long-term use due to their adverse

effects.⁷¹ As a result, new heterocyclic molecules are being developed and a number of them are in the advanced stages of clinical trials.⁷¹ Recently, the utilization of 2-cyano-N-(4-hydroxyphenyl)acetamide has been explored in the construction of fully substituted 2-pyridone derivatives with biomedical features.⁷² In 2021, Fayed and colleagues reported the piperidine-catalyzed three-component reaction of aromatic aldehydes **1**, 2-cyano-N-(4-hydroxyphenyl)acetamide **21b**, and cyanoacetamide **42** in refluxing ethanol for 6 h to afford 2(1*H*)-pyridone derivatives **53a-d** in 58–69% yields (Scheme 15).⁷² This multicomponent approach was successfully extended to ethyl acetoacetate **54** under similar reaction conditions for 2 h to give 2-pyridone derivatives **55a** and **55b** in 81% and 76% yields, respectively. Some compounds were screened for their *in vivo* anti-inflammatory activity employing the carrageenan-stimulated rat hind paw edema method.⁷³ The anti-inflammatory behavior of compounds **53b** ($R = 4\text{-MeOC}_6\text{H}_4$), **53c** ($R = 4\text{-BrC}_6\text{H}_4$), **55a** ($R = 4\text{-MeOC}_6\text{H}_4$), and **55b** ($R = 4\text{-ClC}_6\text{H}_4$) in a 100 mg kg^{-1} ratio with a rat's body weight were compared with the standard Phenylbutazone (100 mg kg^{-1}). In particular, compound **53b** displayed the highest anti-inflammatory activity with a percentage of inhibition of 9.2%, 24.6%, 42.2%, and 40.6% at 1, 2, 3, and 4 hours, respectively, which was only superior to the anti-inflammatory effect of Phenylbutazone at 1 hour (0.72%, 29.9%, 41.2%, and 43.3%, respectively). Lastly, compounds **53b**, **53c**, **55a**, and **55b** were screened for their *in vitro* anti-inflammatory activity using the interleukin-6 kits and Phenylbutazone as a standard drug.⁷⁴ As expected, compound **53b** displayed the highest anti-inflammatory activity with a percentage of IL-6 inhibition of 65.1%, when compared to Phenylbutazone (85.5%). It should be noted that compounds **53c**, **55a**, and **55b** showed a percentage of IL-6 inhibition of 49.5%, 31.4%, and 41.2%, respectively.

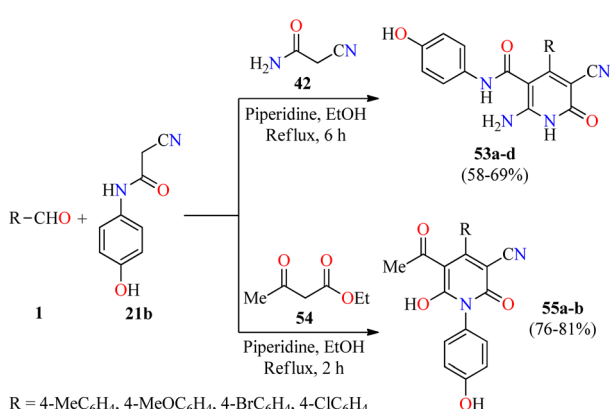
In 2022, the same authors described the piperidine-catalyzed three-component reaction of aromatic aldehydes **1**, 2-cyano-N-(4-hydroxyphenyl)acetamide **21b**, and ethyl acetoacetate **54** or acetylacetone **56** in refluxing ethanol for 2 h to afford fully substituted 2-pyridone derivatives **55a-c** and **57a-c** in 76–87% and 62–89% yields, respectively (Scheme 16).⁷⁵ This



Scheme 16 Three-component synthesis and anti-inflammatory evaluation of 2-pyridone derivatives **55**, **57**, **58**, and **59**.

multicomponent approach was successfully extended to malononitrile **2** or ethyl 2-cyanoacetate **8** under similar reaction conditions for 3–5 h to give 2-pyridone derivatives **58a-f** and **59a-b** in 68–82% and 67–77% yields, respectively. Selected compounds were screened for their *in vivo* anti-inflammatory activity employing the carrageenan-stimulated rat hind paw edema method using Phenylbutazone as a reference drug. In summary, compounds exerted a percentage of inhibition in the range of 10.3–52.6%, 18.4–57.6%, and 27.2–45.6% at 2, 3, and 4 hours, respectively, in comparison to Phenylbutazone (29.9%, 41.2%, and 43.3%, respectively). Most of the tested compounds showed a higher anti-inflammatory effect than Phenylbutazone. Particularly, compounds **58b** ($R = 4\text{-ClC}_6\text{H}_4$) and **58f** ($R = 4\text{-MeOC}_6\text{H}_4$) displayed an excellent percentage of inhibition of (52.6% and 57.6%) and (44.2% and 50.2%) at 2 and 3 hours, respectively. In addition, compounds **58a** ($R = \text{C}_6\text{H}_5$), **58c** ($R = 4\text{-FC}_6\text{H}_4$), and **58f** showed a percentage of inhibition of 44.2%, 44.2%, and 45.6%, respectively, at 4 hour. Lastly, selected compounds were screened for their *in vitro* anti-inflammatory activity using the interleukin-6 kits and Phenylbutazone as a standard drug.⁷⁵ As expected, compound **58f** showed almost the same activity than Phenylbutazone (85.5%) with a percentage of IL-6 inhibition of 85.0%. In addition, compounds **58a** and **58c** showed a good percentage of IL-6 inhibition corresponding to 79.2% and 67.1%, respectively.

Molecular docking studies were performed to investigate the interactions of compound **58f** ($R = 4\text{-MeOC}_6\text{H}_4$) with the active



Scheme 15 Piperidine-catalyzed three-component synthesis of fully substituted 2-pyridone derivatives **53** and **55** with anti-inflammatory activity.



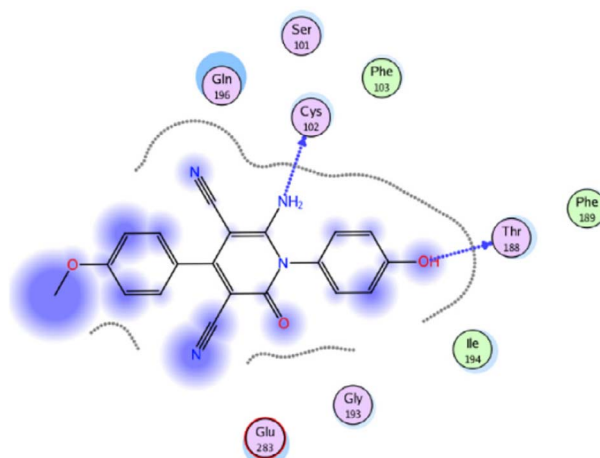
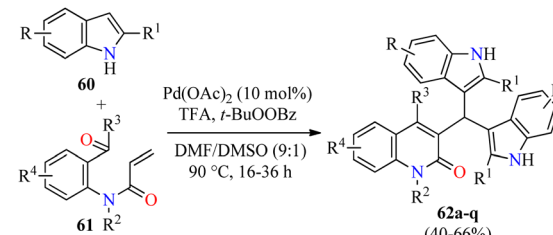


Fig. 6 2D Interactions of compound **58f** with the active site of IL-6 (PDB ID code: 1N26). Reproduced with permission from ref. 75. Copyright Elsevier Inc., 2022.

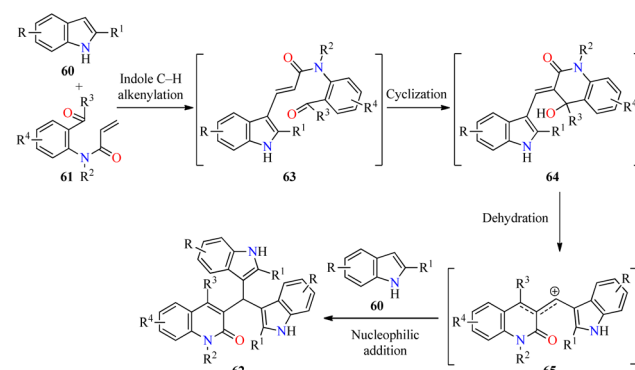
site of IL-6 (PDB ID code: 1N26) (Fig. 6).⁷⁵ The docking research of Phenylbutazone (standard drug) showed that arene–H interaction with Ile194 increased fixation within the active region of IL-6. For compound **58f**, the oxygen atom of the hydroxyl group and nitrogen atom of the amino group formed two H-bonding interactions with Thr188 and Cys102, respectively.

2.5. α -Glucosidase inhibitory activity

Type 2 diabetes is the most common form of diabetes, which is a challenging metabolic disease characterized by insulin resistance, leading to hyperglycemia or abnormal blood glucose levels and damage to various physiological processes and organs.^{76,77} The tremendous increase in the number of patients affected by this disease and the side effects of antidiabetic drugs have promoted the search for new heterocyclic compounds with better safety and antidiabetic activity.^{76,77} In particular, the incorporation of azoles such as pyrazole, imidazole, and triazole, among others, is required in the design of new antihyperglycemic agents with higher activity than acarbose.⁷⁸ Recently, Duan and colleagues reported the cascade synthesis of functionalized 3-bis(indol-3-yl)methylquinoline-2(1H)-ones **62** in 40–66% yields through a pseudo-three-component between indoles **60** and 2-acyl-*N*-acrylaniline derivatives **61** catalyzed by Pd(OAc)₂ (10 mol%) in the presence of an excess of TFA as an additive and TBPP as an oxidant in a mixture of DMF/DMSO (9:1, 3.0 mL) at 90 °C for 16–36 h (Scheme 17).⁷⁹ Notably, three C–C bonds and one ring are formed in one step by Pd-catalyzed C-3 alkenylation of indoles with 2-acyl-*N*-acrylaniline derivatives. Lastly, selected quinolone-bis(indolyl)methane hybrids **62** were screened against α -glucosidase using Acarbose as a reference drug. Most of the compounds showed a higher α -glycosidase inhibition than Acarbose. Remarkably, compounds **62c** ($R = R^1 = R^2 = R^4 = H$, $R^3 = C_6H_5$), **62e** ($R = R^1 = R^3 = R^4 = H$, $R^2 = Bn$), and **62l** ($R = 5\text{-Me}$, $R^1 = R^3 = R^4 = H$, $R^2 = PMB$) showed the highest inhibitory activity with IC_{50} values of 27.5, 21.8, and 15.6 μM , respectively, when compared to Acarbose ($IC_{50} = 154.7 \mu\text{M}$).



Scheme 17 Pd(OAc)₂-Catalyzed pseudo-three-component synthesis of 3-bis(indol-3-yl)methylquinoline-2(1H)-ones **62** as α -glucosidase inhibitors.



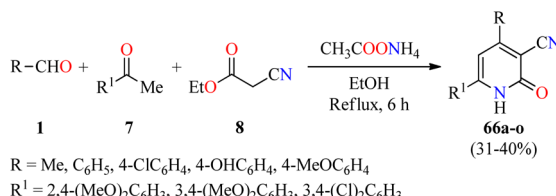
Scheme 18 Plausible mechanism for the synthesis of 3-bis(indol-3-yl)methylquinoline-2(1H)-ones **62**.

As illustrated in Scheme 18, the cascade reaction is triggered by Pd-catalyzed C-3 alkenylation of indoles **60** with 2-acyl-*N*-acrylaniline derivatives **61** to give α,β -unsaturated amides **63**, which underwent an intramolecular cyclization to generate intermediates **64**. The benzylic alcohol moiety of **64** is easily eliminated to form allylic-type carbocations **65**. Lastly, the cascade process is completed by the nucleophilic attack of indoles to the stabilized intermediates **65** to deliver products **62**.

2.6. Cardiotonic activity

Cardiotonic drugs are used for treating cardiac insufficiency because they increase the contractile power of the myocardium improving its capability and efficacy.⁸⁰ In particular, 2-pyridone-based drugs such as Amrinone, Milrinone, and Olprinone have been employed as potent cardiotonic agents during the last decades.^{81–84} In this way, a series of 3-cyano-2(1H)-pyridone derivatives **66** were synthesized through a four-component reaction of aromatic aldehydes **1**, substituted acetophenones **7**, ethyl cyanoacetate **8**, and an excess of ammonium acetate in refluxing ethanol for 6 h (Scheme 19).⁸⁵ The reaction mixture was cooled and the precipitate was filtered, washed successively with water, dried, and recrystallized to afford products **66a–o** in 31–40% yields. These compounds were evaluated for their cardiotonic activity using the spontaneously beating atria model from Reserpine-treated guinea pigs.⁸⁶ Isoproterenol sulfate at a concentration of $5 \times 10^{-4} \text{ M}$ was used as a reference





Scheme 19 Four-component synthesis of 2(1H)-pyridone derivatives 66 as nonsteroidal cardiotonic agents.

standard to be able to follow the changes in both the atria contractility and frequency rate. The best pharmacological profile was obtained with compound 66i ($\text{R} = 4\text{-OHC}_6\text{H}_4, \text{R}^1 = 3,4\text{-}(\text{MeO})_2\text{C}_6\text{H}_3$), which displayed selectivity for increasing the force of contraction (108.7% change over control) rather than the frequency rate (40.8% change over control) at 5×10^{-4} M concentration, in comparison to isoproterenol sulfate (83.7 and 76.4%, respectively).

3 Conclusions and perspectives

2-Pyridone-containing heterocycles play a significant role in drug discovery and medicinal chemistry due to their interesting structural features and a broad range of biological activities. In particular, 2-pyridones can act as bioisosteres for amides; serve as both hydrogen bond donors and/or acceptors; and achieve better drug-like properties such as low lipophilicity, solubility in water, and metabolic stability under physiological conditions. As a result, an increasing number of FDA-approved drugs containing the 2-pyridone motif have been marketed as kinase inhibitors. Most of the preparative routes toward commercial drugs and biologically active compounds involve batch processes and multistep sequences, respectively. To meet the global demand for large-scale manufacturing of higher-value products at a reduced cost, synthetic organic chemists have shifted their attention to continuous flow reactors due to their several advantages over classical batch reactors. In this sense, MCRs can be positively affected by the use of flow processes in terms of yield, selectivity, reaction time, and real-time monitoring. Although there are several 2-pyridone-based drugs and drug candidates, we find very few reports on the multicomponent synthesis of bioactive 2-pyridone derivatives. This review aims to illustrate a variety of MCR-based approaches applied to the synthesis of bioactive 2-pyridone-containing heterocycles, demonstrating the value of this strategy in drug discovery and medicinal chemistry. Although many works have been published on the multistep synthesis of bioactive 2-pyridones, we hope that the reader will gain an appreciation that multicomponent reactions (MCRs) can lead to an overall process with high atom-economy and step-efficiency.

Author contributions

The five individuals listed as authors have contributed substantially to the development of this review, and no other person was involved with its development. The contribution of

authors is as follows: Miss Diana Hurtado-Rodríguez. Papers analysis with anticancer activity and original draw composition. Miss Angélica Salinas-Torres. Papers analysis with anticancer activity and original draw composition. Prof. Dr Hugo Rojas. Manuscript review and editing. Dr Diana Becerra. Papers analysis with anti-inflammatory, α -glucosidase inhibitor, and cardiotonic activities, literature investigation, writing, manuscript review and editing, and conceptualization. Dr Juan-Carlos Castillo. Papers analysis with antibacterial and antifungal activities, literature investigation, writing, manuscript review and editing, conceptualization, and supervision.

Conflicts of interest

There are no conflicts to declare.

Acknowledgements

The authors are grateful for financial support from Universidad Pedagógica y Tecnológica de Colombia. The authors thank to the Dirección de Investigaciones at the Universidad Pedagógica y Tecnológica de Colombia for financial support (project numbers SGI-3073 and SGI-3312).

Notes and references

1. A. Dömling, W. Wang and K. Wang, Chemistry and biology of multicomponent reactions, *Chem. Rev.*, 2012, **112**, 3083–3135.
2. C. G. Neochoritis, T. Zhao and A. Dömling, Tetrazoles *via* multicomponent reactions, *Chem. Rev.*, 2019, **119**, 1970–2042.
3. D. Insuasty, J. Castillo, D. Becerra, H. Rojas and R. Abonia, Synthesis of biologically active molecules through multicomponent reactions, *Molecules*, 2020, **25**, 505.
4. R. Kakuchi, Multicomponent reactions in polymer synthesis, *Angew. Chem., Int. Ed.*, 2014, **53**, 46–48.
5. R. Abonia, J. Castillo, B. Insuasty, J. Quiroga, M. Nogueras and J. Cobo, Efficient catalyst-free four-component synthesis of novel γ -aminoethers mediated by a Mannich type reaction, *ACS Comb. Sci.*, 2013, **15**, 2–9.
6. J. D. Sunderhaus and S. F. Martin, Applications of multicomponent reactions to the synthesis of diverse heterocyclic scaffolds, *Chem. - Eur. J.*, 2009, **15**, 1300–1308.
7. S. E. John, S. Gulati and N. Shankaraiah, Recent advances in multi-component reactions and their mechanistic insights: a triennium review, *Org. Chem. Front.*, 2021, **8**, 4237–4287.
8. D. Becerra, R. Abonia and J.-C. Castillo, Recent applications of the multicomponent synthesis for bioactive pyrazole derivatives, *Molecules*, 2022, **27**, 4723.
9. H. A. Younus, M. Al-Rashida, A. Hameed, M. Uroos, U. Salar, S. Rana and K. M. Khan, Multicomponent reactions (MCR) in medicinal chemistry: a patent review (2010–2020), *Expert Opin. Ther. Pat.*, 2021, **31**, 267–289.
10. A. Strecker, Ueber die künstliche Bildung der Milchsäure und einen neuen, dem glycocoll homologen körper, *Ann. Chem. Pharm.*, 1850, **75**, 27–45.



11 A. Hantzsch, Condensationprodukte aus aldehydammoniak und ketoniartigen verbindungen, *Chem. Ber.*, 1881, **14**, 1637–1638.

12 P. Biginelli, Ueber aldehyduramide des acetessigäthers, *Chem. Ber.*, 1891, **24**, 1317.

13 C. Mannich and W. Krösche, Ueber ein kondensationsprodukt aus formaldehyd, ammoniak und antipyrin, *Arch. Pharm.*, 1912, **250**, 647–667.

14 M. Passerini, Sopra gli isonitrili (I). Composto del *p*-isonitrilazobenzolo con acetone ed acido acetico, *Gazz. Chim. Ital.*, 1921, **51**, 126–129.

15 E. K. Fields, The synthesis of esters of substituted amino phosphonic acids, *J. Am. Chem. Soc.*, 1952, **74**, 1528–1531.

16 F. Asinger, Über die gemeinsame einwirkung von schwefel und ammoniak auf ketone, *Angew. Chem.*, 1956, **68**, 413.

17 I. Ugi, R. Meyr, U. Fetzer and C. Steinbrückner, Versuche mit isonitrilen, *Angew. Chem.*, 1959, **71**, 373–388.

18 K. Gewald, E. Schinke and H. Böttcher, Heterocyclen aus CH-aciden nitrilen, VIII. 2-Amino-thiophene aus methylenaktiven nitrilen, carbonylverbindungen und schwefel, *Chem. Ber.*, 1966, **99**, 94–100.

19 O. H. Oldenziel, D. Van Leusen and A. M. Van Leusen, Chemistry of sulfonylmethyl isocyanides. 13. A general one-step synthesis of nitriles from ketones using tosylmethyl isocyanide. Introduction of a one-carbon unit, *J. Org. Chem.*, 1977, **42**, 3114–3118.

20 H. Bienaymé and K. A. Bouzid, New heterocyclic multicomponent reaction for the combinatorial synthesis of fused 3-aminoimidazoles, *Angew. Chem., Int. Ed.*, 1998, **37**, 2234–2237.

21 R. Abonia, J. Castillo, B. Insuasty, J. Quiroga, M. Nogueras and J. Cobo, An efficient synthesis of 7-(aryl methyl)-3-*tert*-butyl-1-phenyl-6,7-dihydro-1*H*,4*H*-pyrazolo[3,4-*d*][1,3]oxazines, *Eur. J. Org. Chem.*, 2010, **2010**, 6454–6463.

22 A. Boltjes and A. Dömling, The Groebke-Blackburn-Bienaymé reaction, *Eur. J. Chem.*, 2019, **2019**, 7007–7049.

23 M. M. K. Amer, M. A. Aziz, W. S. Shehab, M. H. Abdellatif and S. M. Mouneir, Recent advances in chemistry and pharmacological aspects of 2-pyridone scaffolds, *J. Saudi Chem. Soc.*, 2021, **25**, 101259.

24 S. Sangwan, N. Yadav, R. Kumar, S. Chauhan, V. Dhanda, P. Walia and A. Duhan, A score years' update in the synthesis and biological evaluation of medicinally important 2-pyridones, *Eur. J. Med. Chem.*, 2022, **232**, 114199.

25 S. Lin, C. Liu, X. Zhao, X. Han, X. Li, Y. Ye and Z. Li, Recent advances of pyridinone in medicinal chemistry, *Front. Chem.*, 2022, **10**, 869860.

26 O. Bensaude, M. Chevrier and J. E. Dubois, Lactim-lactam tautomeric equilibria of 2-hydroxypyridines. 1. Cation binding, dimerization, and interconversion mechanism in aprotic solvents. A spectroscopic and temperature-jump kinetic study, *J. Am. Chem. Soc.*, 1978, **100**, 7055–7060.

27 O. Bensaude, M. Chevrier and J. E. Dubois, Lactim/lactam tautomeric interconversion mechanism in water/polar aprotic solvent water systems. 2. Hydration of 2-hydroxypyridines. Evidence for a bifunctional water-

catalyzed proton transfer, *J. Am. Chem. Soc.*, 1979, **101**, 2423–2429.

28 A. Loppinet-Serani, F. Charbonnier, C. Rolando and I. Huc, Role of lactam vs. lactim tautomers in 2(1*H*)-pyridone catalysis of aromatic nucleophilic substitution, *J. Chem. Soc., Perkin Trans. 2*, 1998, **2**, 937–942.

29 Y. Zhang and A. Pike, Pyridones in drug discovery: recent advances, *Bioorg. Med. Chem. Lett.*, 2021, **38**, 127849.

30 C. Laurence, K. A. Brameld, J. Graton, J.-Y. Le Questel and E. Renault, The pK(BHX) database: toward a better understanding of hydrogen-bond basicity for medicinal chemists, *J. Med. Chem.*, 2009, **52**, 4073–4086.

31 G. Yang, Y. Wang, J. Tian and J.-P. Liu, Huperzine A for Alzheimer's disease: a systematic review and meta-analysis of randomized clinical trials, *PLoS One*, 2013, **8**, e74916.

32 R. C. Pandey, M. W. Toussaint, R. M. Stroshane, C. C. Kalita, A. A. Aszalas, A. L. Gawetson, T. T. Wei, K. M. Byrne, R. F. Geoghegan and R. J. White, Fredericamycin A, a new antitumor antibiotic I. Production, isolation and physicochemical properties, *J. Antibiot.*, 1981, **34**, 1389–1401.

33 V. J. Venditto and E. E. Simanek, Cancer therapies utilizing the camptothecins: a review of the *in vivo* literature, *Mol. Pharmaceutics*, 2010, **7**, 307–349.

34 P. Mellini, B. Marrocco, D. Borovika, L. Polletta, I. Carnevale, S. Saladini, G. Stazi, C. Zwergel, P. Trapencieris, E. Ferretti, M. Tafani, S. Valente and A. Mai, Pyrazole-based inhibitors of enhancer of zeste homologue 2 induce apoptosis and autophagy in cancer cells, *Philos. Trans. R. Soc., B*, 2018, **373**, 20170150.

35 E. Vitaku, D. T. Smith and J. T. Njardarson, Analysis of the structural diversity, substitution patterns, and frequency of nitrogen heterocycles among US. FDA approved pharmaceuticals, *J. Med. Chem.*, 2014, **57**, 10257–10274.

36 N. Kerru, L. Gummidi, S. Maddila, K. K. Gangu and S. B. Jonnalagadda, A review on recent advances in nitrogen-containing molecules and their biological applications, *Molecules*, 2020, **25**, 1909.

37 R. Abonia, D. Insuasty, J. Castillo, B. Insuasty, J. Quiroga, M. Nogueras and J. Cobo, Synthesis of novel quinoline-2-one based chalcones of potential anti-tumor activity, *Eur. J. Med. Chem.*, 2012, **57**, 29–40.

38 B. Insuasty, D. Becerra, J. Quiroga, R. Abonia, M. Nogueras and J. Cobo, Microwave-assisted synthesis of pyrimido[4,5-*b*][1,6]naphthyridin-4(3*H*)-ones with potential antitumor activity, *Eur. J. Med. Chem.*, 2013, **60**, 1–9.

39 A. Salinas-Torres, J. Portilla, H. Rojas, D. Becerra and J.-C. Castillo, Synthesis, spectroscopic analysis, and *in vitro* anticancer evaluation of 2-(phenylsulfonyl)-2*H*-1,2,3-triazole, *Molbank*, 2022, **2022**, M1387.

40 A. Salinas-Torres, E. Jiménez, D. Becerra, J. J. Martínez, H. Rojas, J.-C. Castillo and M. A. Macías, Synthesis, anticancer evaluation, thermal and X-ray crystallographic analysis of 2-oxo-2*H*-chromen-7-yl 4-chlorobenzoate using a conductively heated sealed-vessel reactor, *J. Mol. Struct.*, 2023, **1274**, 134414.

41 I. V. Magedov, M. Manpadi, N. M. Evdokimov, E. M. Elias, E. Rozhkova, M. A. Ogasawara, J. D. Bettale,



N. M. Przheval'skii, S. Rogelj and A. Kornienko, Antiproliferative and apoptosis inducing properties of pyrano[3,2-*c*]pyridones accessible by a one-step multicomponent synthesis, *Bioorg. Med. Chem. Lett.*, 2007, **17**, 3872–3876.

42 W. Kemnitzer, J. Drewe, S. Jiang, H. Zhang, Y. Wang, J. Zhao, S. Jia, J. Herich, D. Labreque, R. Storer, K. Meerovitch, D. Bouffard, R. Rej, R. Denis, C. Blais, S. Lamothe, G. Attardo, H. Gourdeau, B. Tseng, S. Kasibhatla and S. X. Cai, Discovery of 4-aryl-4*H*-chromenes as a new series of apoptosis inducers using a cell- and caspase-based high-throughput screening assay. 1. Structure–activity relationships of the 4-aryl group, *J. Med. Chem.*, 2004, **47**, 6299–6310.

43 I. V. Magedov, M. Manpadi, M. A. Ogasawara, A. S. Dhawan, S. Rogelj, S. V. Slambrouck, W. F. A. Steelant, N. M. Evdokimov, P. Y. Uglinskii, E. M. Elias, E. J. Knee, P. Tongwa, M. Y. Antipin and A. Kornienko, Structural simplification of bioactive natural products with multicomponent synthesis. 2. Antiproliferative and antitubulin activities of pyrano[3,2-*c*]pyridones and pyrano[3,2-*c*]quinolones, *J. Med. Chem.*, 2008, **51**, 2561–2570.

44 A. H. Abadi, D. A. Abouel-Ella, J. Lehmann, H. N. Tinsley, B. D. Gary, G. A. Piazza and M. A. O. Abdel-Fattah, Discovery of colon tumor cell growth inhibitory agents through a combinatorial approach, *Eur. J. Med. Chem.*, 2010, **45**, 90–97.

45 A. A. Fadda, K. S. Mohamed, H. M. Refat and E. E. El-Bialy, Synthesis, characterization and biological activity of some novel coumarin derivatives containing pyridine moiety, *Heterocycles*, 2015, **91**, 134–148.

46 M. I. Ansari, A. Arun, M. K. Hussain, R. Konwar and K. Hajela, Discovery of 3,4,6-triaryl-2-pyridones as potential anticancer agents that promote ROS-independent mitochondrial-mediated apoptosis in human breast carcinoma cells, *ChemistrySelect*, 2016, **1**, 4255–4264.

47 J.-C. Castillo, N.-F. Bravo, L.-V. Tamayo, P.-D. Mestizo, J. Hurtado, M. Macías and J. Portilla, Water-compatible synthesis of 1,2,3-triazoles under ultrasonic conditions by a Cu(I) complex-mediated click reaction, *ACS Omega*, 2020, **5**, 30148–30159.

48 M. Sankaran, C. Uvarani, K. Chandraprakash, S. U. Lekshmi, S. Suparna, J. Platts and P. S. Mohan, A regioselective multicomponent protocol for the synthesis of novel bioactive 4-hydroxyquinolin-2(1*H*)-one grafted monospiropyrrolidine and thiapyrrolizidine hybrids, *Mol. Diversity*, 2014, **18**, 269–283.

49 Y. Tangella, K. L. Manasa, V. L. Nayak, M. Sathish, B. Sridhar, A. Alarifi, N. Nagesh and A. Kamal, An efficient one-pot approach for the regio- and diastereoselective synthesis of *trans*-dihydrofuran derivatives: cytotoxicity and DNA-binding studies, *Org. Biomol. Chem.*, 2017, **15**, 6837–6853.

50 E. A. Marwa, M. M. E. Mostafa, M. F. Salwa, A. M. Mona and A. H. Aly, Design, synthesis and docking study of pyridine and thieno[2,3-*b*]pyridine derivatives as anticancer PIM-1 kinase inhibitors, *Bioorg. Chem.*, 2018, **80**, 674–692.

51 I. W. Cheney, S. Yan, T. Appleby, H. Walker, T. Vo, N. Yao, R. Hamatake, Z. Hong and J. Z. Wu, Identification and structure–activity relationships of substituted pyridones as inhibitors of Pim-1 kinase, *Bioorg. Med. Chem. Lett.*, 2007, **17**, 1679–1683.

52 A. C. Pierce, M. Jacobs and C. Stuver-Moody, Docking study yields four novel inhibitors of the protooncogene Pim-1 kinase, *J. Med. Chem.*, 2008, **51**, 1972–1975.

53 M. M. F. Ismail, A. M. Farrag and D. Abou-El-Ela, Synthesis, anticancer screening, and *in silico* ADME prediction of novel 2-pyridones as Pim inhibitors, *J. Heterocycl. Chem.*, 2020, **57**, 3442–3460.

54 T. Mochizuki, C. Kitanaka, K. Noguchi, T. Muramatsu, A. Asai and Y. Kuchino, Physical and functional interactions between Pim-1 kinase and Cdc25A phosphatase. Implications for the Pim-1-mediated activation of the c-Myc signaling pathway, *J. Biol. Chem.*, 1999, **274**, 18659–18666.

55 A. T. A. Boraei, E. H. Eltamany, I. A. I. Ali, S. M. Gebriel and M. S. Nafie, Synthesis of new substituted pyridine derivatives as potent anti-liver cancer agents through apoptosis induction: *in vitro*, *in vivo*, and *in silico* integrated approaches, *Bioorg. Chem.*, 2021, **111**, 104877.

56 C. Walsh, Molecular mechanisms that confer antibacterial drug resistance, *Nature*, 2000, **406**, 775–781.

57 B. Khameneh, M. Iranshahy, V. Soheili and B. S. F. Bazzaz, Review on plant antimicrobials: a mechanistic viewpoint, *Antimicrob. Resist. Infect. Control.*, 2019, **8**, 118.

58 H. H. Jardosh and M. P. Patel, Lanthanum triflate-triggered synthesis of tetrahydroquinazolinone derivatives of *N*-allylquinolone and their biological assessment, *J. Serb. Chem. Soc.*, 2012, **77**, 1561–1570.

59 H. H. Jardosh and M. P. Patel, Microwave-induced CAN promoted atom-economic synthesis of 1*H*-benzo[*b*]xanthene and 4*H*-benzo[*g*]chromene derivatives of *N*-allyl quinolone and their antimicrobial activity, *Med. Chem. Res.*, 2013, **22**, 2954–2963.

60 R. Khajuria, S. Mahajan, Ambica and K. K. Kapoor, Expedited synthesis of coumarin-pyridone conjugates molecules and their anti-microbial evaluation, *J. Chem. Sci.*, 2017, **129**, 1549–1557.

61 A. B. Pandit, M. M. Savant and K. D. Ladva, An efficient one-pot synthesis of highly substituted pyridone derivatives and their antimicrobial and antifungal activity, *J. Heterocycl. Chem.*, 2018, **55**, 983–987.

62 A. Krishna and S. Sarveswari, One-pot synthesis of 2-amino-6-(1,2-dihydro-4-hydroxy-2-oxoquinolin-3-yl)-4-arylpyridine-3-carbonitriles catalysed by NbCl_5 and their *in vitro* antimicrobial studies, *ChemistrySelect*, 2019, **4**, 9987–9992.

63 A. Krishna, V. Vijayakumar and S. Sarveswari, Synthesis of new 3-(2-amino-6-arylpyrimidin-4-yl)-4-hydroxyquinolin-2(1*H*)-ones and their *in vitro* antimicrobial and “DPPH” scavenging activity evaluation, *ChemistrySelect*, 2020, **5**, 7967–7972.

64 M. A. El-Hashash, S. S. Shaban and R. S. Ali, Synthesis of 3-cyano-2-pyridone derivative and its utility in the synthesis of



some heterocyclic compounds with expecting antimicrobial activity, *J. Heterocycl. Chem.*, 2021, **58**, 329–339.

65 E. M. Ahadi, H. Azizian, V. F. Vavasari, A. Aliahmadi, Z. Shahsavari, H. R. Bijanzadeh and S. Balalaie, Synthesis and decarboxylation of functionalized 2-pyridone-3-carboxylic acids and evaluation of their antimicrobial activity and molecular docking, *Iran. J. Pharm. Res.*, 2021, **20**, 456–475.

66 A. Geronikaki, M. Fesatidou, V. Kartsev and F. Macaev, Synthesis and biological evaluation of potent antifungal agents, *Curr. Top. Med. Chem.*, 2013, **13**, 2684–2733.

67 G. Bouz and M. Doležal, Advances in antifungal drug development: an up-to-date mini review, *Pharmaceuticals*, 2021, **14**, 1312.

68 N.-R. Elejalde, M. Macías, J.-C. Castillo, M. Sortino, L. Svetaz, S. Zacchino and J. Portilla, Synthesis and *in vitro* antifungal evaluation of novel *N*-substituted 4-aryl-2-methylimidazoles, *ChemistrySelect*, 2018, **3**, 5220–5227.

69 L. Coussens and Z. Werb, Inflammation and cancer, *Nature*, 2002, **420**, 860–867.

70 K. L. Rock and H. Kono, The inflammatory response to cell death, *Annu. Rev. Pathol.: Mech. Dis.*, 2008, **3**, 99–126.

71 S. Wongrakpanich, A. Wongrakpanich, K. Melhado and J. Rangaswami, A comprehensive review of non-steroidal anti-inflammatory drug use in the elderly, *Aging Dis.*, 2018, **9**, 143–150.

72 E. A. Fayed, A. H. Bayoumi, A. S. Saleh, E. M. E. Al-Arab and Y. A. Ammar, *In vivo* and *in vitro* anti-inflammatory, antipyretic and ulcerogenic activities of pyridone and chromenopyridone derivatives, physicochemical and pharmacokinetic studies, *Bioorg. Chem.*, 2021, **109**, 104742.

73 C. A. Wintere, D. A. Risley and G. W. Nuss, Carrageenin-induced edema in hind paw of the rat as an assay for antiinflammatory drugs, *Proc. Soc. Exp. Biol. Med.*, 1962, **111**, 544–547.

74 M. A. Croce, T. C. Fabian, J. H. Patton, S. M. Melton, M. Moore and L. L. Trenthem, Partial liquid ventilation decreases the inflammatory response in the alveolar environment of trauma patients, *J. Trauma*, 1998, **45**, 273–282.

75 E. A. Fayed, E. M. E. Al-Arab, A. S. Saleh, A. H. Bayoumi and Y. A. Ammar, Design, synthesis, *in silico* studies, *in vivo* and *in vitro* assessment of pyridones and thiazolidinones as anti-inflammatory, antipyretic and ulcerogenic hits, *J. Mol. Struct.*, 2022, **1260**, 132839.

76 L. Suresh, P. Onkara, P. S. V. Kumar, Y. Pydisetty and G. V. P. Chandramouli, Ionic liquid-promoted multicomponent synthesis of fused tetrazolo[1,5-*a*]pyrimidines as α -glucosidase inhibitors, *Bioorg. Med. Chem. Lett.*, 2016, **26**, 4007–4014.

77 A. Chaudhury, C. Duvoor, V. S. R. Dendi, S. Kraleti, A. Chada, R. Ravilla, A. Marco, N. S. Shekhawat, M. T. Montales, K. Kuriakose, A. Sasapu, A. Beebe, N. Patil, C. K. Musham, G. P. Lohani and W. Mirza, Clinical review of antidiabetic drugs: implications for type 2 diabetes mellitus management, *Front. Endocrinol.*, 2017, **8**, 6.

78 M. Özil, M. Emirik, A. Beldüz and S. Ülker, Molecular docking studies and synthesis of novel bisbenzimidazole derivatives as inhibitors of α -glucosidase, *Bioorg. Med. Chem.*, 2016, **24**, 5103–5114.

79 L. Duan, M.-X. Zuo, K.-Q. Xie, Y.-C. Liu, W.-Z. Qiu, L.-P. Wang and S. Liu, Palladium-catalyzed cascade synthesis of novel quinolone-bis(indolyl)methane hybrids as promising α -glucosidase inhibitors, *Synthesis*, 2020, **52**, 1680–1686.

80 A. Y. Bagrov, J. I. Shapiro and O. V. Fedorova, Endogenous cardiotonic steroids: physiology, pharmacology, and novel therapeutic targets, *Pharmacol. Rev.*, 2009, **61**, 9–38.

81 N. A. Klein, S. J. Siskind, W. H. Frishman, E. H. Sonnenblick and T. H. LeJemtel, Hemodynamic comparison of intravenous amrinone and dobutamine in patients with chronic congestive heart failure, *Am. J. Cardiol.*, 1981, **48**, 170–175.

82 R. A. Young and A. Ward, Milrinone: a preliminary review of its pharmacological properties and therapeutic use, *Drugs*, 1988, **36**, 158–192.

83 R. Murakami, K. Sano, Y. Murakami, T. Shimda and S. Morioka, Effects of intracoronary infusion of an inotropic agent, E-1020 (loprinone hydrochloride), on cardiac function: evaluation of left ventricular contractile performance using the end-systolic pressure-volume relationship, *Int. J. Cardiol.*, 1995, **51**, 57–63.

84 A. Abadi, O. Al-Deeb, A. Al-Afify and H. El-Kashef, Synthesis of 4-alkyl(aryl)-6-aryl-3-cyano-2(1*H*)-pyridinones and their 2-imino isosteres as nonsteroidal cardiotonic agents, *Farmaco*, 1999, **54**, 195–201.

85 P. Dorigo, D. Fraccarollo, G. Santostasi, R. M. Gaion, I. Maragno, M. Floreani and F. Carpenedo, Pharmacological characterization of a new milrinone analogue, *Farmaco*, 1994, **49**, 19–23.

86 M. K. Robinson, T. L. Nusair, E. R. Fletcher and H. L. Ritz, A review of the Buehler guinea pig skin sensitization test and its use in a risk assessment process for human skin sensitization, *Toxicology*, 1990, **61**, 91–107.

